Table 4. Incidence of exonic polymorphisms p.P359S and p.N662S, and relative haplotypes in normal controls and 46,XY DSD patients.

Haplotype 359–662	Patients, n = 70	Controls, n = 510	Fisher, p value	OR	OR confidence interval (p = 0.05)
p.359C- p.662A	72.9% (n = 51)	90.6% (n = 462)	p = 0.0001	0.28	0.15–0.51
p.359T- p.662A	0%	1.5% (n = 8)	p = 0.60	0.42	0.02–7.35
p.359C- p.662G	7.1% (n = 5)	0.8% (n = 9)	p = 0.02	4.28	1.39–13.17
p.359T- p.662G (S-S polymorphism)	20% (n = 14)	6% (n = 31)	p = 0.0003	3.86	1.94–7.70

Controls are combined with the published series (matched for ethnicity of patients and controls) [13] [14]. The χ-square test was performed. When combining all patients with the p.662G polymorphism whatever the p.359 allele, this p.662G was significantly more frequent in 46,XY DSD patients: 27.1% (n = 19) vs. 6.8% (n = 40), $p = 0.0001$.

doi:10.1371/journal.pone.0032505.t004

Regarding severe 46,XY DSD with uncertain sex, only one published paper to date has reported three *MAMLD1* mutations (p.E124X, p.Q197X and p.R653X) [15]. It is precisely in this situation of severe genital malformation that the diagnosis of the causative mechanism is of clinical interest for medical treatment (hormone substitution, pubertal follow-up). In order to determine whether this report was an exceptional observation or of practical clinical interest, we screened 70 patients with severe 46,XY DSD of unknown origin. We identified two new mutations of *MAMLD1* in patients with severe hypospadias and microphallus (1 stop codon and 1 missense mutation). These mutations were associated with a severe phenotype, and reduced (p.P384L) or abolished (p.S143X) transactivation function was found in two cases. 46,XY DSD with normal *AR*, *SRD5A2* and *NR5A1*gene sequences can thus reveal a mutation of *MAMLD1*. This finding suggests a new diagnostic investigation for these patients and may be helpful in genetic counselling if a mutation is identified. It also provides new insight into the pathophysiology of DSD. Indeed, in the family of the child bearing the p.S143X mutation, the mother was heterozygous and two other males on the maternal side of the family exhibited a consistent phenotype. Unfortunately, the family declined any further investigation.

The mechanisms by which these mutations with reduced transactivation induce DSD are still under investigation. As noted above, several studies have provided strong evidence of *MAMLD1* implication in fetal sex development through modulation of testosterone production at the time of sex differentiation. The plasma testosterone measured in one of our cases was indeed lowered but it was normal in the other one, as previously reported in patients with nonsense mutations [15]. Plasma testosterone evaluation is thus not systematically helpful in orienting the diagnosis of DSD since mutations of the genes implicated in testosterone production - such as *MAMLD1* and *NR5A1* - have been reported in 46,XY DSD patients with normal plasma testosterone. These findings, along with the absence of correlation between the *in vitro* functional analysis and the biological and clinical phenotype, suggest that the genital malformation is primarily related to a transient prenatal testicular (Leydig cell) dysfunction and the resulting compromised testosterone production around the critical period of sex differentiation [33]. In the postnatal period, the mouse homolog of *MAMLD1* was indeed reported to be weakly expressed in the testis at one week of age and the expression was faint thereafter.

We also report a high incidence of the rare haplotype p.P359S-p.N662S in our series. The p.P359S (which was designated p.P286S in the previous report) variant was first reported in a patient with hypospadias but it was absent in his brother and nephew with the same phenotype [15]. The p.N662S (which was designated p.P589S in the previous report) variant was found in hypospadiac patients but was also reported in a normal population, although with low incidence [15]. We and others have found that the S-S haplotype is associated with a minor form of DSD, i.e., isolated hypospadias [14], but the *in vitro* functional study of the p.P359S-p.N662S *MAMLD1* variant was inconclusive with unchanged transactivation function [13]. In the present study, we show that the combination of these alleles was present in as much as 15% of patients with severe 46,XY DSD. This is significantly higher than in the controls [combining the series, 15% (n = 70) vs. 10.7% (n = 510), $p = 0.0003$]. Again, a transient testosterone production failure during prenatal development may have contributed to the undervirilization of the external genitalia, but how this haplotype can be present in normal, mild and severe phenotypes remains to be elucidated.

Severe undervirilization in XY newborns can reveal mutations of *MAMLD1*. *MAMLD1* should be routinely sequenced in these patients with otherwise normal *AR*, *SRD5A2* and *NR5A1* genes.

Acknowledgments

We would like to thank Dr Béroud (Laboratoire de Génétique Chromosomique, Institut Universitaire de Recherche Clinique, Université de Montpellier 1, France) for his great help in the statistical study of haplotypes.

Author Contributions

Conceived and designed the experiments: NK MF CS TO PP. Performed the experiments: NK MF PP FA. Analyzed the data: NK MF PP FA CP JW GP SM MP. Contributed reagents/materials/analysis tools: CP JW GP SM MP. Wrote the paper: NK TO CS PP FA.

References

1. Thyen U, Lanz K, Holterhus PM, Hiort O (2006) Epidemiology and initial management of ambiguous genitalia at birth in Germany. Horm Res 66: 195–203.
2. Nelson P (2007) Epidemiology of Hypospadias. Dialogues in Pediatric Urology 28: 2–3.
3. Paulozzi LJ, Erickson JD, Jackson RJ (1997) Hypospadias trends in two US surveillance systems. Pediatrics 100: 831–834.
4. Martinez-Frias ML, Prieto D, Prieto L, Bermejo E, Rodriguez-Pinilla E, et al. (2004) Secular decreasing trend of the frequency of hypospadias among newborn male infants in Spain. Birth Defects Res A Clin Mol Teratol 70: 75–81.
5. Fisch H, Hyun G, Hensle TW (2010) Rising hypospadias rates: disproving a myth. J Pediatr Urol 6: 37–39.
6. Lin L, Philibert P, Ferraz-de-Souza B, Kelberman D, Homfray T, et al. (2007) Heterozygous missense mutations in steroidogenic factor 1 (SF1/Ad4BP,

NR5A1) are associated with 46,XY disorders of sex development with normal adrenal function. J Clin Endocrinol Metab 92: 991–999.
7. Coutant R, Mallet D, Lahlou N, Bouhours-Nouet N, Guichet A, et al. (2007) Heterozygous mutation of steroidogenic factor-1 in 46,XY subjects may mimic partial androgen insensitivity syndrome. J Clin Endocrinol Metab 92: 2868–2873.
8. Morel Y, Rey R, Teinturier C, Nicolino M, Michel-Calemard L, et al. (2002) Aetiological diagnosis of male sex ambiguity: a collaborative study. Eur J Pediatr 161: 49–59.
9. Choi J, Kim G, Seo E, KS K, Kim S, et al. (2008) Molecular analysis of the AR and SRD5A2 genes in patients with 46,XY disorders of sex development. J Pediatr Endocrinol Metab 21: 545–553.
10. Laporte J, Kioschis P, Hu LJ, Kretz C, Carlsson B, et al. (1997) Cloning and characterization of an alternatively spliced gene in proximal Xq28 deleted in two patients with intersexual genitalia and myotubular myopathy. Genomics 41: 458–462.
11. Bartsch O, Kress W, Wagner A, Seemanova E (1999) The novel contiguous gene syndrome of myotubular myopathy (MTM1), male hypogenitalism and deletion in Xq28:report of the first familial case. Cytogenet Cell Genet 85: 310–314.
12. Hu LJ, Laporte J, Kress W, Kioschis P, Siebenhaar R, et al. (1996) Deletions in Xq28 in two boys with myotubular myopathy and abnormal genital development define a new contiguous gene syndrome in a 430 kb region. Hum Mol Genet 5: 139–143.
13. Kalfa N, Cassorla F, Audran F, Oulad Abdennabi I, Philibert P, et al. (2011) Polymorphisms of MAMLD1 gene in hypospadias. J Pediatr Urol 7: 585–591.
14. Chen Y, Thai HT, Lundin J, Lagerstedt-Robinson K, Zhao S, et al. (2010) Mutational study of the MAMLD1-gene in hypospadias. Eur J Med Genet 53: 122–126.
15. Fukami M, Wada Y, Miyabayashi K, Nishino I, Hasegawa T, et al. (2006) CXorf6 is a causative gene for hypospadias. Nat Genet 38: 1369–1371.
16. Quigley CA, French FS (1994) Androgen insensitivity syndromes. Curr Ther Endocrinol Metab 5: 342–351.
17. Kalfa N, Liu B, Ophir K, Audran F, Wang MH, et al. (2008) Mutations of CXorf6 are associated with a range of severities of hypospadias. Eur J Endocrinol 159: 453–458.
18. Philibert P, Audran F, Pienkowski C, Morange I, Kohler B, et al. (2010) Complete androgen insensitivity syndrome is frequently due to premature stop codons in exon 1 of the androgen receptor gene: an international collaborative report of 13 new mutations. Fertil Steril 94: 472–476.
19. Maimoun L, Philibert P, Cammas B, Audran F, Bouchard P, et al. (2010) Phenotypical, Biological, and Molecular Heterogeneity of 5{alpha}-Reductase Deficiency: An Extensive International Experience of 55 Patients. J Clin Endocrinol Metab 96: 296–307.
20. Philibert P, Leprieur E, Zenaty D, Thibaud E, Polak M, et al. (2010) Steroidogenic factor-1 (SF-1) gene mutation as a frequent cause of primary amenorrhea in 46,XY female adolescents with low testosterone concentration. Reprod Biol Endocrinol 8: 28.
21. Cole C, Barber JD, Barton GJ (2008) The Jpred 3 secondary structure prediction server. Nucleic Acids Res 36: W197–201.
22. Petersen B, Petersen TN, Andersen P, Nielsen M, Lundegaard C (2009) A generic method for assignment of reliability scores applied to solvent accessibility predictions. BMC Struct Biol 9: 51.
23. Kelley LA, Sternberg MJ (2009) Protein structure prediction on the Web: a case study using the Phyre server. Nat Protoc 4: 363–371.
24. Ramensky V, Bork P, Sunyaev S (2002) Human non-synonymous SNPs: server and survey. Nucleic Acids Res 30: 3894–3900.
25. Thomas PD, Kejariwal A (2004) Coding single-nucleotide polymorphisms associated with complex vs. Mendelian disease: evolutionary evidence for differences in molecular effects. Proc Natl Acad Sci U S A 101: 15398–15403.
26. Mi H, Dong Q, Muruganujan A, Gaudet P, Lewis S, et al. (2010) PANTHER version 7: improved phylogenetic trees, orthologs and collaboration with the Gene Ontology Consortium. Nucleic Acids Res 38: D204–210.
27. Kumar P, Henikoff S, Ng PC (2009) Predicting the effects of coding non-synonymous variants on protein function using the SIFT algorithm. Nat Protoc 4: 1073–1081.
28. Yue P, Melamud E, Moult J (2006) SNPs3D: candidate gene and SNP selection for association studies. BMC Bioinformatics 7: 166.
29. Fukami M, Wada Y, Okada M, Kato F, Katsumata N, et al. (2008) Mastermind-like domain containing 1 (MAMLD1 or CXorf6) transactivates the Hes3 promoter, augments testosterone production, and contains the SF1 target sequence. J Biol Chem 29: 5525–5532.
30. Nishimura M, Isaka F, Ishibashi M, Tomita K, Tsuda H, et al. (1998) Structure, chromosomal locus, and promoter of mouse Hes2 gene, a homologue of Drosophila hairy and Enhancer of split. Genomics 49: 69–75.
31. Sadovsky Y, Dorn C (2000) Function of steroidogenic factor 1 during development and differentiation of the reproductive system. Rev Reprod 5: 136–142.
32. Ogata T, Laporte J, Fukami M (2009) MAMLD1 (CXorf6): a new gene involved in hypospadias. Horm Res 71: 245–252.
33. Welsh M, MacLeod DJ, Walker M, Smith LB, Sharpe RM (2010) Critical androgen-sensitive periods of rat penis and clitoris development. Int J Androl 33: e144–152.
34. Shibata Y, Kojima Y, Mizuno K, Nakane A, Kato T, et al. Optimal cutoff value of contralateral testicular size for prediction of absent testis in Japanese boys with nonpalpable testis. Urology 76: 78–81.

OPEN ACCESS Freely available online

PLoS one

Identification of Novel Low-Dose Bisphenol A Targets in Human Foreskin Fibroblast Cells Derived from Hypospadias Patients

Xian-Yang Qin[1,2], Yoshiyuki Kojima[3], Kentaro Mizuno[3], Katsuhiko Ueoka[4], Koji Muroya[5], Mami Miyado[6], Hiroko Zaha[1], Hiromi Akanuma[1], Qin Zeng[1], Tomokazu Fukuda[7], Jun Yoshinaga[2], Junzo Yonemoto[1], Kenjiro Kohri[3], Yutaro Hayashi[3], Maki Fukami[6], Tsutomu Ogata[6,8], Hideko Sone[1]*

1 Health Risk Research Section, Research Center for Environmental Risk, National Institute for Environmental Studies, Tsukuba, Ibaraki, Japan, **2** Department of Environmental Studies, Graduate School of Frontier Science, The University of Tokyo, Kashiwa, Chiba, Japan, **3** Department of Nephro-Urology, Nagoya City University Graduate School of Medical Sciences, Nagoya, Aichi, Japan, **4** Department of Surgical Subspecialties, National Research Center for Child Health and Development, Tokyo, Japan, **5** Division of Endocrinology and Metabolism, Kanagawa Children's Medical Center, Kanagawa, Yokohama, Japan, **6** Department of Endocrinology and Metabolism, National Research Institute for Child Health and Development, Tokyo, Japan, **7** Department of Animal Production Science, Graduate School of Agricultural Science, Tohoku University, Sendai, Miyagi, Japan, **8** Department of Pediatrics, University Hospital, Hamamatsu University School of Medicine, Hamamatsu, Shizuoka, Japan

Abstract

Background/Purpose: The effect of low-dose bisphenol A (BPA) exposure on human reproductive health is still controversial. To better understand the molecular basis of the effect of BPA on human reproductive health, a genome-wide screen was performed using human foreskin fibroblast cells (hFFCs) derived from child hypospadias (HS) patients to identify novel targets of low-dose BPA exposure.

Methodology/Principal Findings: Gene expression profiles of hFFCs were measured after exposure to 10 nM BPA, 0.01 nM 17β-estradiol (E2) or 1 nM 2,3,7,8-tetrachlorodibenzo-p-dioxin (TCDD) for 24 h. Differentially expressed genes were identified using an unpaired Student's t test with *P* value cut off at 0.05 and fold change of more than 1.2. These genes were selected for network generation and pathway analysis using Ingenuity Pathways Analysis, Pathway Express and KegArray. Seventy-one genes (42 downregulated and 29 upregulated) were identified as significantly differentially expressed in response to BPA, among which 43 genes were found to be affected exclusively by BPA compared with E2 and TCDD. Of particular interest, real-time PCR analysis revealed that the expression of matrix metallopeptidase 11 (MMP11), a well-known effector of development and normal physiology, was found to be inhibited by BPA (0.47-fold and 0.37-fold at 10 nM and 100 nM, respectively). Furthermore, study of hFFCs derived from HS and cryptorchidism (CO) patients ($n=23$ and 11, respectively) indicated that MMP11 expression was significantly lower in the HS group than in the CO group (0.25-fold, $P=0.0027$).

Conclusions/Significance: This present study suggests that an involvement of BPA in the etiology of HS might be associated with the downregulation of MMP11. Further study to elucidate the function of the novel target genes identified in this study during genital tubercle development might increase our knowledge of the effects of low-dose BPA exposure on human reproductive health.

Citation: Qin X-Y, Kojima Y, Mizuno K, Ueoka K, Muroya K, et al. (2012) Identification of Novel Low-Dose Bisphenol A Targets in Human Foreskin Fibroblast Cells Derived from Hypospadias Patients. PLoS ONE 7(5): e36711. doi:10.1371/journal.pone.0036711

Editor: Bin He, Baylor College of Medicine, United States of America

Received March 6, 2012; **Accepted** April 12, 2012; **Published** May 4, 2012

Funding: This study was supported by the Ministry of the Environment, Japan, and by a grant for Research on Risk on Chemical Substances (H20-004) from the Ministry of Health, Labour and Welfare, Japan (http://www.mhlw.go.jp/english/index.html). The funders had no role in the study design, data collection and analysis, decision to publish, or preparation of the manuscript.

Competing Interests: The authors have declared that no competing interests exist.

* E-mail: hsone@nies.go.jp

Introduction

Hypospadias (HS) is one of the most common congenital abnormalities with a global prevalence of approximately 0.2–1% at birth in male infants [1]. The etiology of HS is poorly understood, and might include genetic, hormonal and environmental factors. It has been hypothesized that testicular cancer, cryptorchidism (CO) and some cases of HS and impaired spermatogenesis are symptoms of a single underlying entity that has been named as the testicular dysgenesis syndrome (TDS) [2,3]. This concept proposes the existence of a common underlying cause for the occurrence of these reproductive and developmental diseases, and suggests that adverse environmental factors, such as environmental endocrine disruptors (EEDs) might exert their etiological effects on a susceptible genetic background.

Bisphenol A (BPA) is one of the world's highest production-volume chemicals, with more than six billion pounds produced worldwide each year [4]. BPA is used extensively in the plastics produced for food and beverage containers, such as baby bottles,

plastic containers and the resin lining of cans [4]. Among the known estrogen-like EEDs, BPA has received much attention because it is commonly found in the environment as well as in human tissues and fluids (1–19.4 nM) [4,5]. BPA has been detected in 92% of urine samples in a US reference population, suggesting people may be continuously exposed to this compound in their daily lives [6]. The US Food and Drug Administration and Environmental Protection Agency concluded in the 1980s that a daily dose of 50 μg/kg/day was safe for humans, which is currently considered as $<2.19\times10^{-7}$ M for *in vitro* cell or organ culture studies [7]. However, in recent decades, there has been a heated controversy over the safety of BPA among scientists and risk assessors.

Recently, exposure to BPA at concentrations detected in humans has been reported to affect neurological, cardiovascular and metabolic diseases (such as diabetes), and even cancers [8–12]. However, the effect of low-dose BPA exposure on human reproductive health is still controversial [13,14]. Li *et al.* reported that occupational exposure to BPA has adverse effects on male sexual dysfunction, which is the first evidence that exposure to BPA in the workplace could have an adverse effect on male sexual dysfunction [15]. Jasarevic *et al.* reported that exposure to BPA at low doses can affect sexual behaviors, even with no changes in sexual phenotypes or hormones [16]. Furthermore, Zhang *et al.* reported that low-dose BPA exposure could directly disrupt steroidogenesis in human cells [17]. It seems that exposure to BPA might affect human reproductive health by complicated mechanisms that encompass more than just estrogen receptor (ER) mediated pathways.

In this study, to better understand the molecular basis of the effects of BPA on human reproductive health, a genome-wide screen was performed using human foreskin fibroblast cells (hFFCs) derived from child HS patients to identify novel targets of low-dose BPA exposure. Furthermore, the effect of BPA on the global gene expression profile of hFFCs was compared with that of 17β-estradiol (E2) and 2,3,7,8-tetrachlorodibenzo-p-dioxin (TCDD), which are representative agonists of ER and aryl hydrocarbon receptor (AhR) signaling pathways, respectively.

Materials and Methods

Samples

hFFCs from child HS ($n=23$; median age 2.3 yrs) and CO ($n=11$; median age 2.3 yrs) patients undergoing surgical procedures were obtained from the National Research Institute for Child Health and Development, Japan, during 2007–2009. All subjects were of Japanese origin and written informed consent was obtained from the guardians on the behalf of the children participants involved in this study. This study was approved by the Institutional Ethics Committees of the Nagoya City University Graduate School of Medical Sciences, the National Research Institute for Child Health and Development and the National Institute for Environmental Studies.

Table 1. Summary of genes differentially expressed in response to BPA, E2 and TCDD.

	BPA		E2		TCDD	
P-value	1.0-fold	1.2-fold	1.0-fold	1.2-fold	1.0-fold	1.2-fold
0.05	154	71*	1101	814*	1150	824*
0.01	30	17	198	154	208	156
0.001	7	5	16	11	14	9

*Selected as significant differentially expressed genes and used for the network generation and pathway analysis.
doi:10.1371/journal.pone.0036711.t001

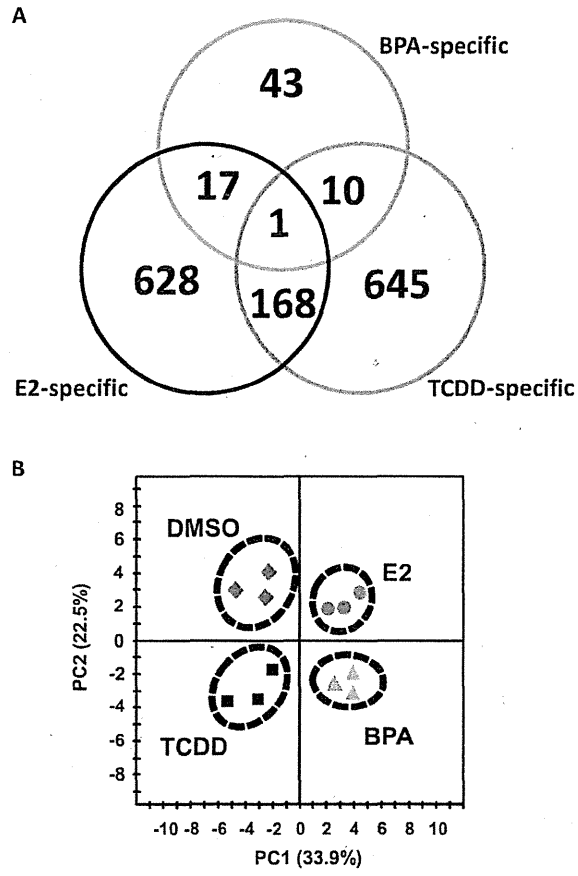

Figure 1. Genetic response of hFFCs to BPA, E2 and TCDD. (*A*) Venn-diagrams showing the number of genes that were considered significantly deregulated among the three treatment groups. (*B*) PCA scoreplot from transcript data of three hFFC cultures treated with DMSO, 10 nM BPA, 0.01 nM E2 and 1 nM TCDD.
doi:10.1371/journal.pone.0036711.g001

Chemicals

Dimethyl sulfoxide (DMSO) and E2 were obtained from Sigma Chemical Co. (St. Louis, MO, USA). BPA was obtained from Wako Industries (Osaka, Japan) and TCDD was obtained from Cambridge Isotope Laboratories (Cambridge, MA, USA). DMSO was used as the primary solvent for all chemicals, and the DMSO solutions were further diluted in cell culture media for treatments. The final concentrations of DMSO in media did not exceed 0.1% (vol/vol).

Cell culture

hFFCs were maintained in Dulbecco's Modified Eagle Medium (DMEM)/Ham's F-12 (048-29785, Wako, Osaka, Japan) containing 10% fetal bovine serum (FBS, Mediatech, Herndon, VA, USA) and grown at 37°C in a 5% CO_2 humidified incubator. For growth under steroid-free conditions, cells were seeded in phenol red-free DMEM/Ham's F-12 (045-30665, Wako) containing 5%

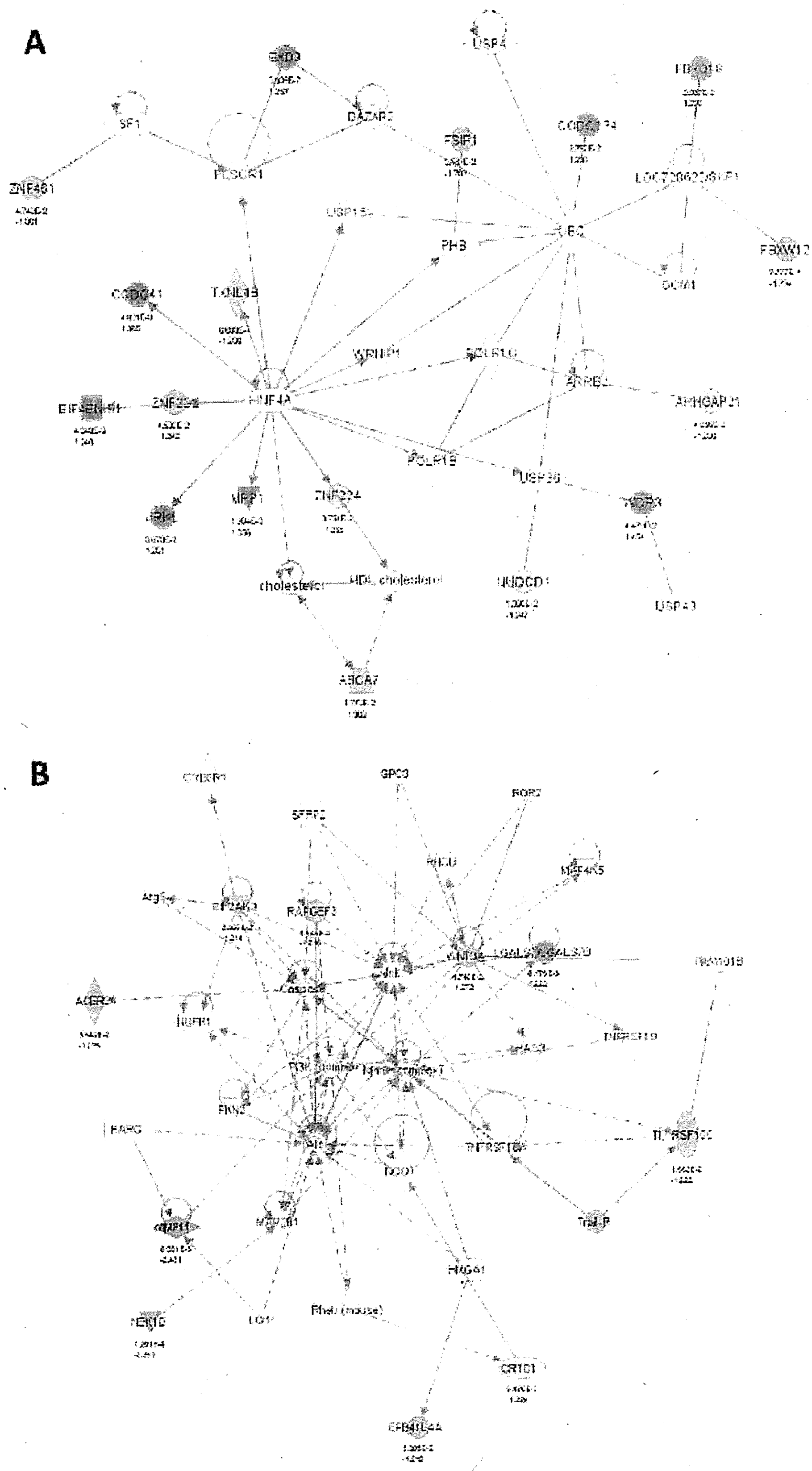
A
HNF4A
PHB
FBXW12
cholesterol
HDL cholesterol
ABCA7
B
Akt
HMGA1

Figure 2. Network associated genes differentially expressed in response to BPA. (*A*) "Endocrine System Disorders, Gastrointestinal Disease, Genetic Disorder" network and (*B*) "Cell Death, Cellular Growth and Proliferation, Cancer" network. The images were created using the IPA platform by overlaying the differentially expressed genes in response to BPA detected by Agilent microarray analysis onto a global molecular network from the Ingenuity knowledgebase. Red indicates upregulated genes, green indicates downregulated genes, and white indicates genes that were not annotated in this array but that form part of this network. The bottom numbers indicate the fold changes induced by BPA, and the top numbers are the *P*-values between the DMSO control group and the BPA treated group. Direct relationships are exhibited with solid arrows and indirect relationships with dashed arrows.
doi:10.1371/journal.pone.0036711.g002

charcoal/dextran-treated FBS (Hyclone, Logan, UT, USA). All culture media contained 100 U/ml penicillin/streptomycin and 2 mmol/L L-glutamine (Mediatech, Herndon, VA, USA).

RNA isolation and DNA microarray analysis

Total RNA was isolated from cultured cells after treatment with chemicals for 24 h using an RNeasy Kit (Qiagen, Valencia, CA, USA) in accordance with the manufacturer's instructions. Quantification and quality assessment of the isolated RNA samples were performed and verified using an Agilent Bioanalyzer2100 (Agilent Technologies, Palo Alto, CA, USA) and a NanoDrop spectrophotometer (NanoDrop products, Wilmington, DE, USA) in accordance with the manufacturer's instructions. RNA was amplified into cRNA and labeled according to the Agilent One-Color Microarray-Based Gene Expression Analysis protocol (Agilent Technologies). Samples were then hybridized to G4851A SurePrint G3 Human GE 8×60K array slides (60,000 probes, Agilent Technologies). The slides were processed according to the manufacturer's instructions without any modification. The arrays were scanned using an Agilent Microarray Scanner (G2565BA, Agilent Technologies).

MIAME

All data are MIAME compliant, and the raw data have been deposited in the Gene Expression Omnibus (www.ncbi.nlm.nih.gov/geo, accession no. GSE35034).

Array data analysis

The scanned images were analyzed using the standard procedures described in the Agilent Feature Extraction software 9.5.3.1 (Agilent Technologies). Data analysis was performed with GeneSpring GX12.0.2 (Agilent Technologies). Signal intensities for each probe were normalized to the 75th percentile without baseline transformation. Genes that were differentially expressed following chemical treatments were identified by the unpaired Student's t test with P values cut off at 0.05 and fold change of more than 1.2 and were used for the network generation and pathway analysis.

Network generation and pathway analysis

The Ingenuity Pathways Analysis (IPA) program (Ingenuity Systems, Mountain View, CA, USA; http://www.ingenuity.com) was used to identify networks and canonical pathways of genes differentially expressed in response to BPA, E2 and TCDD. IPA software uses an extensive database of functional interactions that are drawn from peer-reviewed publications and manually maintained [18]. For the IPA analysis, the Agilent SurePrint G3 Human GE 8×60 K Array was used as a reference gene set. The generated biological networks were ranked by score, which is the likelihood of a set of genes being found in the networks owing to random chance, identified by a Fisher's exact test. The generated canonical pathways were ranked by P values, which is calculated using a Fisher's exact test by comparing the number of user-specified genes of interest that participate in a given function or pathway, relative to the total number of occurrences of these genes in all functional/pathway annotations stored in the Ingenuity

Table 2. Top five associated network functions of genes differentially expressed in response to BPA, E2 and TCDD generated by IPA.

Chemical	Top Functions	Score
BPA	Endocrine System Disorders, Gastrointestinal Disease, Genetic Disorder	41
	Cell Death, Cellular Growth and Proliferation, Cancer	21
	Cellular Growth and Proliferation, Hematological System Development and Function, Cellular Development	18
	Cellular Assembly and Organization, Cellular Function and Maintenance, Cell Cycle	13
	Dermatological Diseases and Conditions, Inflammatory Disease	3
E2	Cellular Growth and Proliferation, Skeletal and Muscular System Development and Function, Cell Cycle	41
	DNA Replication, Recombination, and Repair, Gene Expression, Cellular Assembly and Organization	41
	Cellular Assembly and Organization, Cellular Function and Maintenance, Protein Synthesis	41
	Gene Expression, Cell Cycle, Cell-To-Cell Signaling and Interaction	35
	DNA Replication, Recombination, and Repair, Nucleic Acid Metabolism, Small Molecule Biochemistry	33
TCDD	Post-Translational Modification, Genetic Disorder, Hematological Disease	49
	Cell Cycle, Cellular Assembly and Organization, DNA Replication, Recombination, and Repair	47
	Cellular Assembly and Organization, DNA Replication, Recombination, and Repair, Decreased Levels of Albumin	45
	DNA Replication, Recombination, and Repair, Energy Production, Nucleic Acid Metabolism	44
	DNA Replication, Recombination, and Repair, Cell Cycle, Cellular Assembly and Organization	37

doi:10.1371/journal.pone.0036711.t002

Table 3. Top canonical pathways for genes differentially expressed in response to BPA, E2 and TCDD identified by IPA.

Chemical	Top canonical pathway	P-Value
BPA	RAN Signaling	5.31E-02
	Endoplasmic Reticulum Stress Pathway	6.34E-02
	Leukocyte Extravasation Signaling	1.24E-01
	Retinoic acid Mediated Apoptosis Signaling	1.54E-01
	Colorectal Cancer Metastasis Signaling	1.93E-01
E2	Cell Cycle: G1/S Checkpoint Regulation	1.01E-03
	PI3K/AKT Signaling	1.52E-03
	Role of NFAT in Regulation of the Immune Response	1.83E-03
	p53 Signaling	3.46E-03
	Aryl Hydrocarbon Receptor Signaling	3.63E-03
TCDD	Cell Cycle Control of Chromosomal Replication	1.20E-09
	Role of BRCA1 in DNA Damge Response	1.72E-07
	Mismatch Repair in Eukaryotes	2.47E-05
	Hereditary Breast Cancer Signaling	9.45E-04
	Role of CHK Proteins in Cell Cycle Checkpoint Control	1.00E-02

doi:10.1371/journal.pone.0036711.t003

Pathways Knowledge Base [19]. In addition, genes significantly differentially expressed in response to BPA, E2 and TCDD was analyzed by Pathway Express (http://vortex.cs.wayne.edu/projects.htm) and mapped to Kyoto Encyclopedia of Genes and Genomes (KEGG) pathways by KegArray (http://www.kegg.jp/kegg/download/kegtools.html).

Quantitative real-time reverse-transcription polymerase chain reaction (RT-PCR)

cDNA was synthesized using a High Capacity RNA-to-cDNA Kit (Applied Biosystems, Foster City, CA, USA) according to the manufacturer's instructions. Real-time PCR was performed using TaqMan® Gene Expression Master Mix (Applied Biosystems) in accordance with the manufacturer's instructions. TaqMan® Gene Expression Assays (Applied Biosystems) used in this study were: Hs02341150_m1 for POMZP3, Hs01094348_m1 for WDR3, Hs00171829_m1 for metallopeptidase 11 (MMP11; see gene names in Table S1), and Hs00266705 g1 for glyceraldehyde-3-phosphate dehydrogenase (GAPDH). The primers (Forward: 5′-TGTTGGGGGATAAGGACAAA-3′; and Reverse: 5′-GCAGGCTGTACAGGAACCAT-3′) and probe (5′-TAAACT-CACCTCTGTGGTTGGAACAAT-3′) for NEK10 were designed and synthesized by Hokkaido System Science (Sapporo, Hokkaido, Japan). The amplification reaction was performed in an ABI PRISM 7000 Sequence Detector (Applied Biosystems) under the following cycling conditions: 95°C for 15 min, followed by 40 cycles of 95°C for 15 s and 60°C for 60 s. The gene expression levels were calculated based on the threshold cycle using Sequence Detection System Software (Applied Biosystems). Gene expression was normalized to that of GAPDH and set to 100 for the control DMSO-treated cells.

Statistical and multivariate analysis

Quantitative data were expressed as the mean ± SEM. A nonparametric test, the Mann-Whitney U test, was applied to test for statistical significance. Values of $P<0.05$ were considered to indicate statistical significance. Unsupervised principal component analysis (PCA) was run in SIMCA-P+ (Version 12.0, Umetrics, Umeå, Sweden) to obtain a general overview of the variance of genes differentially expressed in response to BPA, E2 and TCDD.

Results

Gene expression profiles of hFFCs in response to BPA, E2 and TCDD

The gene expression profiles in hFFCs treated with DMSO control or 10 nM BPA, 0.01 nM E2 or 1 nM TCDD were determined by Agilent microarray analysis using three biological replicates. Then, differentially expressed genes in response to BPA, E2 and TCDD compared with DMSO control were identified by the unpaired Student's t test with P values cut off at 0.05 and fold change of more than 1.2 using GeneSpring GX software. Seventy-one genes (42 downregulated and 29 upregulated), 814 genes (371 downregulated and 443 upregulated), and 824 genes (344 downregulated and 480 upregulated) were identified to be significantly differentially expressed in response to BPA, E2, and TCDD, respectively. No nuclear receptor was found to be significantly differentially expressed in response to BPA, while estrogen-related receptor-α (ESRRA), retinoic acid receptor-α (RARA) and RAR-related orphan receptor-α (RORA) and RARA were found to be significantly differentially expressed in response to E2 and TCDD, respectively. The summary of differentially expressed genes along with their P values and fold changes is provided in Table 1.

Differences in the response of hFFCs to BPA, E2 and TCDD

Comparison of the gene expression profiles of hFFCs in response to BPA, E2 and TCDD is provided in Figure 1. BPA-specific responses were found in 43 significantly differentially expressed genes, compared with responses to E2 and TCDD (Figure 1A). Seventeen and 10 differentially expressed genes were found to be common in response to BPA with E2 or TCDD, respectively. A full list of these genes is summarized in Table S1.

Furthermore, to compare the expression patterns of hFFCs in response to BPA with that of E2 or TCDD, PCA analysis was performed on the data of significantly differentially expressed genes in response to BPA. PCA is a standard technique of pattern recognition and multivariate data analysis. Of interest, the cells treated with DMSO, BPA, E2 and TCDD were clearly distinguished from each other by the PCA score plots (Figure 1B). According to the first component (PC1), which represents 33.9% of the total variance, a very clear discrimination between cells treated with BPA or E2 and those treated with DMSO or TCDD was observed. However, according to the second component (PC2), which represents 22.5% of the total variance, cells treated with BPA or TCDD were clearly distinguished from those treated with DMSO or E2. It should be noted that differences in the PCA were identified using an unsupervised analysis, without any prior information on the samples. Since all cells were cultured under identical conditions, the observed discriminations demonstrate that the effect of BPA is similar to that of E2 according to PC1 but is similar to that of TCDD according to PC2.

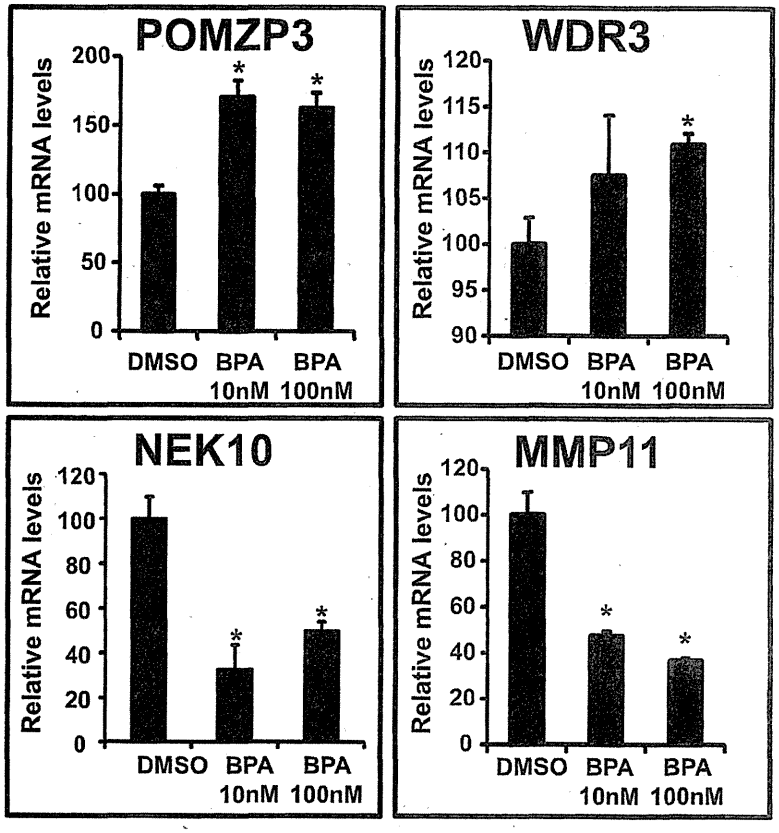

Figure 3. Validation of POMZP1, WDR3, NEK10 and MMP11 expression. Cells were treated with BPA at 10 nM and 100 nM for 24 h, and then the expression of POMZP1, WDR3, NEK10 and MMP11 was examined by real-time PCR. *$P<0.05$ vs. DMSO control cells.
doi:10.1371/journal.pone.0036711.g003

Network generation and pathway analysis of genes differentially expressed in response to BPA, E2 and TCDD

To investigate possible biological interactions of differently regulated genes, datasets derived from microarray analysis representing genes with altered expression profiles were imported into the IPA platform. Network analysis of the biological functions of the top five IPA-generated networks is summarized in Table 2 and is shown in Figure 2 and Figure S1,S2,S3.The two most highly populated biological networks entitled "Endocrine System Disorders, Gastrointestinal Disease, Genetic Disorder" (Score = 41) and "Cell Death, Cellular Growth and Proliferation, Cancer" (Score = 21) were identified with genes differentially expressed in response to BPA (Figure 2). The networks consisted of genes that encoded enzymes (ACER2, PLSCR1, POLR1C, TXNL4B and UBC), peptidases (MMP11, UCHL5, USP4, USP36 and USP43), proteins that regulate transcription (ABCA7, CRTC1, HNF4A, LOC728622/SKP1, PHB, SF1 and SLC25A6) and translation (EIF4ENIF1 and TNFRSF10C), and others (ARHGAP21, ARRB2, CCDC41, CCDC134, EIF2AK3, EPB41L4A, DAZAP2, EPB41L3, EXD3, FBXO18, FBXW12, FSIP1, JRKL, LGALS7/LGALS7B, NEK10, NUDCD1, RAPGEF3, SERPINA1, WDR3, WNT3A, ZNF222, ZNF224 and ZNF461). The most highly populated biological networks were identified with genes differentially expressed in response to E2 and TCDD and were entitled "Cellular Growth and Proliferation, Skeletal and Muscular System Development and Function, Cell Cycle" (Score = 41) and "Post-Translational Modification, Genetic Disorder, Hematological Disease" (Score = 49), respectively. Furthermore, top canonical pathways associated with genes significantly differentially expressed in response to BPA, E2 and TCDD were summarized in Table 3. The pathway most affected by BPA is "RAN Signaling" with only borderline significance ($P = 0.0531$). The pathways most affected by E2 and TCDD are "Cell Cycle: G1/S Checkpoint Regulation" and "Cell Cycle Control of Chromosomal Replication", respectively ($P = 1.01\times10^{-3}$ and 1.20×10^{-9}, respectively).

In addition, a list of top KEGG pathways affected by BPA, E2 and TCDD identified by Pathway Express was summarized in Table S2. By inputting the list of genes significantly differentially expressed in response to BPA, E2 and TCDD into Pathway Express, 12 KEGG pathways, but without statistical significance, were found to be affected by BPA, while 27 and 9 KEGG pathways were found to be significantly affected by E2 and TCDD, respectively. As an example, "Pathways in cancer" of KEGG mapped with genes significantly differentially expressed in response to BPA, E2 and TCDD using KegArray was illustrated in Figure S4.

Validation by real-time PCR

To validate the microarray data and to identify potential biomarkers for BPA toxicity in hFFCs derived from HS patients, the expression of the most up- or down-regulated genes (POMZP3, 1.46-fold; WDR3, 1.45-fold; NEK10, 0.44-fold;

A

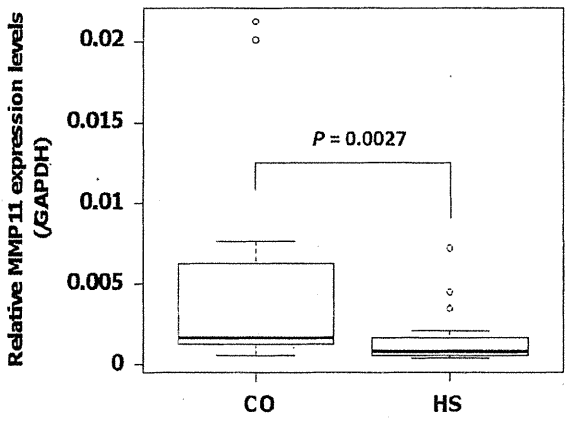

B

	n	Relative MMP11 expression levels (/GAPDH) (mean ± SEM)
CO	11	0.0058 ± 0.0022
HS	23	0.0015 ± 0.00033

Figure 4. Reduced levels of MMP11 expression in hFFCs derived from child HS patients. Significantly lower MMP11 expression was observed in hFFCs derived from the HS ($n = 23$) group compared with the CO ($n = 11$) group by TaqMan real-time PCR. (*A*) Boxplot and (*B*) summary of the quantitative data comparing MMP11 expression levels in HS and CO groups.
doi:10.1371/journal.pone.0036711.g004

MMP11, 0.41-fold) in response to BPA was validated by real-time PCR. As the results show in Figure 3, the PCR data showed good concordance with the microarray data in terms of the expression direction (up- or down-regulation). A significant increase in the mRNA levels of POMZP3 and WDR3 and a significant decrease in the mRNA levels of NEK10 and MMP11 were observed following BPA treatments at high and/or low concentrations (10 nM and 100 nM, respectively).

Comparison of MMP11 expression levels in hFFCs derived from child HS and CO patients

To further investigate the potential role of MMP11 in the development of HS, we examined the expression levels of MMP11 in hFFCs derived from child HS and CO patients ($n = 23$ and 11, respectively). As shown Figure 4, the mean MMP11 expression level, normalized to GAPDH, in the HS group was 0.0015 and in the CO group, 0.0058. Significantly lower MMP11 expression levels were observed in the HS group compared with the CO group (0.25-fold, $P = 0.0027$).

Discussion

To better understand the molecular basis of the effects of BPA on human reproductive health, target genes of low-dose BPA exposure were identified in hFFCs derived from child HS patients using DNA microarray analysis. Human foreskin tissues obtained from patients with HS have been used as *in vitro* models to define the etiology of HS [20–22]. However, these investigations have not delineated the relative contribution of environmental factors. To our knowledge, our study is the first report to use hFFCs to investigate the potential effects of BPA on the development of HS. The concentration of BPA used to treat the cells in our microarray analysis was 10 nM, which is below the dose of 50 μg/kg/day (approximately 200 nM for *in vitro* cell or organ culture studies) usually considered as safe for humans [7]. Moreover, this dose is in the concentration range of 1–19.4 nM that is commonly detected in human tissues and fluids [4].

In this study, we compared the gene expression profiles of hFFCs in response to BPA, E2 and TCDD. Using PCA, we found that the effect of BPA is similar to that of E2 according to PC1 but is similar to that of TCDD according to PC2. Forty-three genes were found to be affected exclusively by BPA, underscoring the concept that the effects observed are ER and AhR-independent (Figure 1). In our previous study, we examined the estrogenic activity of BPA in estrogen receptor 1 (ESR1)-positive BG1Luc4E2 human ovarian cancer cells and found that BPA increased the ESR1-induced luciferase activity in a dose-dependent manner with a lowest observed effect at 100 nM [23]. Although differences exist between cell lines, it is possible that the underlying mechanisms of the endocrine-disrupting effects of BPA at doses lower than the reference limits might involve pathways other than estrogen signaling. Indeed, differences in transcript profiles in response to BPA and E2 have been previously described in ESR1-positive human cells [24]. Furthermore, amore recent study reported that BPA might lead to severe malformation during vertebrate embryogenesis, while no effects were seen with exposure to the E2 or ER-antagonist ICI 182,780 [25].

It is not unexpected that the largest biological network identified by IPA analysis with genes differentially expressed in response to BPA was entitled "Endocrine System Disorders, Gastrointestinal Disease, Genetic Disorder" (Table 2 and Figure 2A). It should be noted that this network contains three genes (ZNF222, ZNF224 and ZNF461) that belong to the zinc finger protein (ZFP) family. ZFPs are among the most abundant proteins in eukaryotic genomes and play various roles in the regulation of transcription [26]. The biological function of ZNF222 and ZNF461 remains to be investigated, but ZNF224 participates in key cellular processes, such as regulation of cell growth [27]. Previous reports have revealed that ZNF224 might play a critical role in bladder carcinogenesis by regulating the apoptosis of bladder cancer cells [28]. None of these three ZNFs have been previously associated with the development of HS. However, two other zinc finger box genes, ZEB1 and ZEB2, have been associated with HS [20,29]. Our data indicate that ZFP-mediated transcriptional activity might be required for the effect of BPA on human reproduction. It is known that zinc finger structures are as diverse as their functions [26]. Therefore, it is likely that further investigations into the function of ZFPs in transcriptional regulation will provide novel insights to explain the association we found between ZFP expression and low-dose BPA exposure regarding the pathogenesis of HS.

The expression of four of the significantly differentially expressed genes identified in the microarray analysis was verified by real-time PCR analysis. Of particular interest, MMP11 (0.47-fold and 0.37-fold at 10 nM and 100 nM, respectively), which is involved in the "Cell Death, Cellular Growth and Proliferation, Cancer" network, was shown to be down-regulated (Figures 2B and 3). The matrix metalloproteinases (MMPs) are zinc-dependent endopeptidases that are involved in the breakdown of extracellular matrix (ECM) in normal physiological processes, such as embryonic development, reproduction, and tissue remodeling, as well as in disease processes, such as arthritis and metastasis [30,31]. It is well known that MMP11 is overexpressed in several human cancers, including breast, cervix, colon, ovary, prostate,

and stomach cancers [30,32–34]. Several MMPs have been implicated in ECM degradation associated with tumor growth and angiogenesis, which is required for a cancer cell to invade a nearby blood vessel (intravasation) and then to extravasate at a distant location and invade the distant tissue in order to seed a new metastatic site [35].

To our knowledge, there have not been any reports of human congenital genital disorders associated with MMP11. However, it has been reported that MMPs play a critical role in cell fate and behavior during many developmental processes [31,36]. Both genetic analysis using transgenic mice and pharmacogenetic studies with chemical inhibitors have elucidated that loss of function of MMPs, in particular MMP11, might induce dysregulation in cell migration and apoptosis during tissue remodeling or branching of mammary epithelial cells [37,38]. A more recent study in the model insect, *Tribolium*, explored MMP functions *in vivo* and found that knockdown of MMPs using genetic interference resulted in malformation in tracheal and gut development during beetle embryogenesis and pupal morphogenesis [39]. It is known that epithelial seam formation and remodeling during urethral formation play important roles in the etiology of HS. The urethral abnormalities seen in HS can be viewed as a failure of epithelial cell adhesion [40]. Therefore, we hypothesized that downregulation of MMP11 expression might decrease cellular adhesion in the developing male urethra and ventral penile skin, which might result in the abortive penile development seen in HS.

To further confirm this hypothesis, we compared the expression levels of MMP11 in hFFCs derived from child HS and CO patients ($n = 23$ and 11, respectively). In 2001, Skakkebaek and his colleagues proposed a concept of TDS: impaired development of fetal testes could lead to increased risks of CO, HS, decreased spermatogenesis or testicular cancer [2]. However, they have recently changed their opinion and now suggest that HS is only marginally associated with TDS [3]. Although much remains to be determined, it is likely that the molecular etiology of HS and CO is different. CO is the absence of one or both testes from the scrotum and is the most common congenital abnormality in boys with a reported prevalence at birth of approximately 2–9%, according to registry data [41]. Impaired descent of the testes is thought to be fetal in origin, and if the *in utero* development of the testicles is impaired then their production of insulin-like factor 3 and especially testosterone may be reduced, which may lead to some degree of CO [3,42]. However, it is likely that isolated HS may have a different etiological mechanism, including a congenital developmental problem restricted to the penis [43]. Rey *et al.* found that most boys (85%) with isolated HS had, in general, normal testicular endocrinology in contrast to those with HS combined with other genital abnormalities [44]. In this study, only child HS and CO patients without other genital malformations of syndromes were recruited. Therefore, hFFCs derived from foreskin tissues of child CO patients might be viewed as the control group in this study. We found that MMP11 expression in the HS group was significantly lower than in the CO group (0.25-fold, $P = 0.0027$) (Figure 4). This result is in accordance with our hypothesis that downregulation of MMP11 expression might be related with the pathology of HS. Although the urethral tissue was not directly examined, it is possible that there is also a potential effect of MMP11 on urethral development.

In summary, the present study examined targets of low-dose BPA exposure and transcriptome differences in response to BPA, E2 and TCDD in hFFCs derived from child HS patients using DNA microarray analysis. Of particular interest, the expression of MMP11 was found to be downregulated by BPA in a dose-dependent manner. Furthermore, we also found that MMP11 expression in the HS group was significantly lower than in the CO group. Our findings suggested that the involvement of BPA in the development of HS might relate to downregulation of MMP11 expression. Further study of the novel target genes identified in this study during genital tubercle development might increase our knowledge of the molecular basis of the effects of BPA on human reproductive health.

Supporting Information

Figure S1 Red indicates upregulated genes, green indicates downregulated genes, and white indicates genes that were not annotated in this array but form part of this network. The bottom numbers indicate the fold changes induced by BPA and the top numbers is the P-values between DMSO control group and BPA treated group. (***A***) "Cellular Growth and Proliferation, Hematological System Development and Function, Cellular Development" network; (***B***) "Cellular Assembly and Organization, Cellular Function and Maintenance, Cell Cycle" network.
(DOCX)

Figure S2 Red indicates upregulated genes, green indicates downregulated genes, and white indicates genes that were not annotated in this array but form part of this network. The bottom numbers indicate the fold changes induced by E2 and the top numbers is the P-values between DMSO control group and E2 treated group. (***A***) "Cellular Growth and Proliferation, Skeletal and Muscular System Development and Function, Cell Cycle" network; (***B***) "DNA Replication, Recombination, and Repair, Gene Expression, Cellular Assembly and Organization" network; (***C***) "Cellular Assembly and Organization, Cellular Function and Maintenance, Protein Synthesis" network; (***D***) "Gene Expression, Cell Cycle, Cell-To-Cell Signaling and Interaction" network; (***E***) "DNA Replication, Recombination, and Repair, Nucleic Acid Metabolism, Small Molecule Biochemistry" network.
(DOCX)

Figure S3 Red indicates upregulated genes, green indicates downregulated genes, and white indicates genes that were not annotated in this array but form part of this network. The bottom numbers indicate the fold changes induced by TCDD and the top numbers is the P-values between DMSO control group and TCDD treated group. (***A***) "Post-Translational Modification, Genetic Disorder, Hematological Disease" network; (***B***) "Cell Cycle, Cellular Assembly and Organization, DNA Replication, Recombination, and Repair" network; (***C***) "Cellular Assembly and Organization, DNA Replication, Recombination, and Repair, Decreased Levels of Albumin" network; (***D***) "DNA Replication, Recombination, and Repair, Energy Production, Nucleic Acid Metabolism" network; (***E***) "DNA Replication, Recombination, and Repair, Cell Cycle, Cellular Assembly and Organization" network.
(DOCX)

Figure S4 "Pathways in cancer" of KEGG was mapped with genes significantly differentially expressed in response to BPA (*A*), E2 (*B*) and TCDD (*C*).
(DOCX)

Table S1 Comparison of the gene expression profiles of hFFCs in response to BPA, E2 and TCDD.
(DOCX)

Table S2 KEGG pathways affected by BPA, E2 and TCDD identified by Pathway Express.
(DOCX)

Acknowledgments

The authors gratefully acknowledge critical advices of Dr. Jun Kanno (National Institute of Health Sciences, Japan) and Dr. Yasunobu Aoki (National Institute for Environmental Studies, Japan).

Author Contributions

Conceived and designed the experiments: TF J. Yoshinaga J. Yonemoto MF TO HS. Performed the experiments: XYQ HZ HA QZ. Analyzed the data: XYQ. Contributed reagents/materials/analysis tools: YK K. Mizuno KU K. Muroya MM KK YH MF TO. Wrote the paper: XYQ HS.

References

1. Toppari J, Virtanen HE, Main KM, Skakkebaek NE (2010) Cryptorchidism and hypospadias as a sign of testicular dysgenesis syndrome (TDS): environmental connection. Birth Defects Res A Clin Mol Teratol 88: 910–919.
2. Skakkebaek NE, Rajpert-De Meyts E, Main KM (2001) Testicular dysgenesis syndrome: an increasingly common developmental disorder with environmental aspects. Hum Reprod 16: 972–978.
3. Jorgensen N, Meyts ER, Main KM, Skakkebaek NE (2010) Testicular dysgenesis syndrome comprises some but not all cases of hypospadias and impaired spermatogenesis. Int J Androl 33: 298–303.
4. Vandenberg LN, Hauser R, Marcus M, Olea N, Welshons WV (2007) Human exposure to bisphenol A (BPA). Reprod Toxicol 24: 139–177.
5. Krishnan AV, Stathis P, Permuth SF, Tokes L, Feldman D (1993) Bisphenol-A: an estrogenic substance is released from polycarbonate flasks during autoclaving. Endocrinology 132: 2279–2286.
6. Calafat AM, Kuklenyik Z, Reidy JA, Caudill SP, Ekong J, et al. (2005) Urinary concentrations of bisphenol A and 4-nonylphenol in a human reference population. Environ Health Perspect 113: 391–395.
7. Wetherill YB, Akingbemi BT, Kanno J, McLachlan JA, Nadal A, et al. (2007) In vitro molecular mechanisms of bisphenol A action. Reprod Toxicol 24: 178–198.
8. Allard P, Colaiacovo MP (2010) Bisphenol A impairs the double-strand break repair machinery in the germline and causes chromosome abnormalities. Proc Natl Acad Sci U S A 107: 20405–20410.
9. Leranth C, Hajszan T, Szigeti-Buck K, Bober J, MacLusky NJ (2008) Bisphenol A prevents the synaptogenic response to estradiol in hippocampus and prefrontal cortex of ovariectomized nonhuman primates. Proc Natl Acad Sci U S A 105: 14187–14191.
10. Lang IA, Galloway TS, Scarlett A, Henley WE, Depledge M, et al. (2008) Association of urinary bisphenol A concentration with medical disorders and laboratory abnormalities in adults. JAMA 300: 1303–1310.
11. Wei J, Lin Y, Li Y, Ying C, Chen J, et al. (2011) Perinatal exposure to bisphenol A at reference dose predisposes offspring to metabolic syndrome in adult rats on a high-fat diet. Endocrinology 152: 3049–3061.
12. Qin XY, Fukuda T, Yang L, Zaha H, Akanuma H, et al. (2012) Effects of bisphenol A exposure on the proliferation and senescence of normal human mammary epithelial cells. Cancer Biol Ther 13.
13. Sharpe RM (2010) Is it time to end concerns over the estrogenic effects of bisphenol A? Toxicol Sci 114: 1–4.
14. Welshons WV, Nagel SC, vom Saal FS (2006) Large effects from small exposures. III. Endocrine mechanisms mediating effects of bisphenol A at levels of human exposure. Endocrinology 147: S56–69.
15. Li D, Zhou Z, Qing D, He Y, Wu T, et al. (2010) Occupational exposure to bisphenol-A (BPA) and the risk of self-reported male sexual dysfunction. Hum Reprod 25: 519–527.
16. Jasarevic E, Sieli PT, Twellman EE, Welsh TH, Jr., Schachtman TR, et al. (2011) Disruption of adult expression of sexually selected traits by developmental exposure to bisphenol A. Proc Natl Acad Sci U S A 108: 11715–11720.
17. Zhang X, Chang H, Wiseman S, He Y, Higley E, et al. (2011) Bisphenol A disrupts steroidogenesis in human H295R cells. Toxicol Sci 121: 320–327.
18. Calvano SE, Xiao W, Richards DR, Felciano RM, Baker HV, et al. (2005) A network-based analysis of systemic inflammation in humans. Nature 437: 1032–1037.
19. Bronner IF, Bochdanovits Z, Rizzu P, Kamphorst W, Ravid R, et al. (2009) Comprehensive mRNA expression profiling distinguishes tauopathies and identifies shared molecular pathways. PLoS One 4: e6826.
20. Qiao L, Tasian GE, Zhang H, Cunha GR, Baskin L (2011) ZEB1 is estrogen responsive in vitro in human foreskin cells and is over expressed in penile skin in patients with severe hypospadias. J Urol 185: 1888–1893.
21. Vottero A, Minari R, Viani I, Tassi F, Bonatti F, et al. (2011) Evidence for epigenetic abnormalities of the androgen receptor gene in foreskin from children with hypospadias. J Clin Endocrinol Metab 96: E1953–1962.
22. Wang Z, Liu BC, Lin GT, Lin CS, Lue TF, et al. (2007) Up-regulation of estrogen responsive genes in hypospadias: microarray analysis. J Urol 177: 1939–1946.
23. Qin XY, Zaha H, Nagano R, Yoshinaga J, Yonemoto J, et al. (2011) Xenoestrogens down-regulate aryl-hydrocarbon receptor nuclear translocator 2 mRNA expression in human breast cancer cells via an estrogen receptor alpha-dependent mechanism. Toxicol Lett 206: 152–157.
24. Singleton DW, Feng Y, Yang J, Puga A, Lee AV, et al. (2006) Gene expression profiling reveals novel regulation by bisphenol-A in estrogen receptor-alpha-positive human cells. Environ Res 100: 86–92.
25. Gibert Y, Sassi-Messai S, Fini JB, Bernard L, Zalko D, et al. (2011) Bisphenol A induces otolith malformations during vertebrate embryogenesis. BMC Dev Biol 11: 4.
26. Laity JH, Lee BM, Wright PE (2001) Zinc finger proteins: new insights into structural and functional diversity. Curr Opin Struct Biol 11: 39–46.
27. Lupo A, Cesaro E, Montano G, Izzo P, Costanzo P (2011) ZNF224: Structure and role of a multifunctional KRAB-ZFP protein. Int J Biochem Cell Biol 43: 470–473.
28. Harada Y, Kanehira M, Fujisawa Y, Takata R, Shuin T, et al. (2010) Cell-permeable peptide DEPDC1-ZNF224 interferes with transcriptional repression and oncogenicity in bladder cancer cells. Cancer Res 70: 5829–5839.
29. Garavelli L, Cerruti-Mainardi P, Virdis R, Pedori S, Pastore G, et al. (2005) Genitourinary anomalies in Mowat-Wilson syndrome with deletion/mutation in the zinc finger homeo box 1B gene (ZFHX1B). Report of three Italian cases with hypospadias and review. Horm Res 63: 187–192.
30. Peruzzi D, Mori F, Conforti A, Lazzaro D, De Rinaldis E, et al. (2009) MMP11: a novel target antigen for cancer immunotherapy. Clin Cancer Res 15: 4104–4113.
31. Vu TH, Werb Z (2000) Matrix metalloproteinases: effectors of development and normal physiology. Genes Dev 14: 2123–2133.
32. Valdivia A, Peralta R, Matute-Gonzalez M, Garcia Cebada JM, Casasola I, et al. (2011) Co-expression of metalloproteinases 11 and 12 in cervical scrapes cells from cervical precursor lesions. Int J Clin Exp Pathol 4: 674–682.
33. McCord LA, Li F, Rosewell KL, Brannstrom M, Curry TE, Jr. (2011) Ovarian Expression and Regulation of the Stromelysins During the Periovulatory Period in the Human and the Rat. Biol Reprod.
34. Desmedt C, Majjaj S, Kheddoumi N, Singhal SK, Haibe-Kains B, et al. (2012) Characterization and Clinical Evaluation of CD10+ Stroma Cells in the Breast Cancer Microenvironment. Clin Cancer Res 18: 1004–1014.
35. Roy R, Yang J, Moses MA (2009) Matrix metalloproteinases as novel biomarkers and potential therapeutic targets in human cancer. J Clin Oncol 27: 5287–5297.
36. Wei L, Shi YB (2005) Matrix metalloproteinase stromelysin-3 in development and pathogenesis. Histol Histopathol 20: 177–185.
37. Ishizuya-Oka A, Li Q, Amano T, Damjanovski S, Ueda S, et al. (2000) Requirement for matrix metalloproteinase stromelysin-3 in cell migration and apoptosis during tissue remodeling in Xenopus laevis. J Cell Biol 150: 1177–1188.
38. Simian M, Hirai Y, Navre M, Werb Z, Lochter A, et al. (2001) The interplay of matrix metalloproteinases, morphogens and growth factors is necessary for branching of mammary epithelial cells. Development 128: 3117–3131.
39. Knorr E, Schmidtberg H, Vilcinskas A, Altincicek B (2009) MMPs regulate both development and immunity in the tribolium model insect. PLoS One 4: e4751.
40. Baskin LS, Erol A, Jegatheesan P, Li Y, Liu W, et al. (2001) Urethral seam formation and hypospadias. Cell Tissue Res 305: 379–387.
41. Virtanen HE, Bjerknes R, Cortes D, Jorgensen N, Rajpert-De Meyts E, et al. (2007) Cryptorchidism: classification, prevalence and long-term consequences. Acta Paediatr 96: 611–616.
42. Kojima Y, Mizuno K, Kohri K, Hayashi Y (2009) Advances in molecular genetics of cryptorchidism. Urology 74: 571–578.
43. Kojima Y, Kohri K, Hayashi Y (2010) Genetic pathway of external genitalia formation and molecular etiology of hypospadias. J Pediatr Urol 6: 346–354.
44. Rey RA, Codner E, Iniguez G, Bedecarras P, Trigo R, et al. (2005) Low risk of impaired testicular Sertoli and Leydig cell functions in boys with isolated hypospadias. J Clin Endocrinol Metab 90: 6035–6040.

RESEARCH ARTICLE

AMERICAN JOURNAL OF medical genetics PART A

Complex Genomic Rearrangement in the *SOX9* 5′ Region in a Patient With Pierre Robin Sequence and Hypoplastic Left Scapula

Maki Fukami,[1]* Takayoshi Tsuchiya,[1,2] Shuji Takada,[3] Akiko Kanbara,[4] Hiroshi Asahara,[3] Arisa Igarashi,[3] Yasunori Kamiyama,[4] Gen Nishimura,[5] and Tsutomu Ogata[1,6]

[1]Department of Molecular Endocrinology, National Research Institute for Child Health and Development, Tokyo, Japan

[2]Department of Pediatrics, Dokkyo Medical University, Koshigaya Hospital, Koshigaya, Japan

[3]Department of Systems BioMedicine, National Research Institute for Child Health and Development, Tokyo, Japan

[4]Department of Pediatrics, Saiseikai Utsunomiya Hospital, Utsunomiya, Japan

[5]Department of Pediatric Imaging, Tokyo Metropolitan Children's Medical Center, Tokyo, Japan

[6]Department of Pediatrics, Hamamatsu University School of Medicine, Hamamatsu, Japan

Manuscript Received: 28 November 2011; Manuscript Accepted: 3 February 2012

Pierre Robin sequence (PRS) can occur as a component of campomelic dysplasia (CD) and acampomelic CD (ACD) caused by dysfunction or dysregulation of SOX9, although it can also take place as an isolated form. Recently, genomic alterations in the far upstream and the far downstream region of *SOX9* have been identified in patients with isolated PRS. Here, we report on a male patient with PRS and a heterozygous genomic rearrangement in the 5′ region of *SOX9*. Clinical analysis revealed PRS-compatible craniofacial anomalies, mild hypoplasia of the left scapula, and normal male external genitalia. Molecular analysis identified a paracentric inversion on the long arm of chromosome 17 with breakpoints at 17q21.31 and 17q24.3, and a microdeletion spanning from −4.15 to −1.16 Mb relative to *SOX9*. These findings indicate that the chromosomal region more than 1.16 Mb apart from *SOX9* contains at least one developmental enhancer(s) for *SOX9* that plays a critical role in the development of the mandible and a relatively small role in the development of the scapula. Moreover, the concept of exclusion mapping argues that putative CD/ACD loci are located within the 1.16 Mb region closest to *SOX9* coding exons, which remain intact in this Non-CD/ACD patient. This study provides a novel example for long-range *cis*-regulatory mutations of *SOX9*. © 2012 Wiley Periodicals, Inc.

Key words: campomelic dysplasia; deletion; inversion; enhancer; noncoding element

How to Cite this Article:
Fukami M, Tsuchiya T, Takada S, Kanbara A, Asahara H, Igarashi A, Kamiyama Y, Nishimura G, Ogata T. 2012. Complex genomic rearrangement in the *SOX9* 5′ region in a patient with Pierre Robin sequence and hypoplastic left scapula.
Am J Med Genet Part A 158A:1529–1534.

INTRODUCTION

Pierre Robin sequence (PRS) (OMIM 261800) is a congenital malformation sequence characterized by micrognathia, glossoptosis, and posterior U-shaped cleft palate [Robin, 1934]. The primary defect of PRS is assumed to be mandibular hypoplasia caused by impaired chondrogenesis or aberrant proliferation of neural crest cells [Gordon et al., 2009]. PRS frequently occurs as a component of known syndromes such as campomelic dysplasia (CD) (OMIM 114290), acampomelic CD (ACD), and Stickler syndrome (OMIM 108300), although PRS can also take place as an isolated (nonsyndromic) form [Holder-Espinasse et al., 2001].

Grant sponsor: Ministry of Education, Culture, Sports, Science and Technology (MEXT); Grant number: 22132004; Grant sponsor: Japan Society for the Promotion of Science (JSPS); Grant number: 23390249; Grant sponsor: Ministry of Health, Labor and Welfare; Grant numbers: 10103415, 11103332; Grant sponsor: National Center for Child Health and Development; Grant number: 23A-1.
Maki Fukami, Takayoshi Tsuchiya, and Shuji Takada contributed equally to this work.
The authors have no conflict of interest.
*Correspondence to:
Maki Fukami, MD, Department of Molecular Endocrinology, National Research Institute for Child Health and Development, 2-10-1 Ohkura, Setagaya, Tokyo 157-8535, Japan. E-mail: mfukami@nch.go.jp
Article first published online in Wiley Online Library (wileyonlinelibrary.com): 23 April 2012
DOI 10.1002/ajmg.a.35308

CD and ACD are caused by dysfunction or dysregulation of SOX9; multiple intragenic mutations of *SOX9* as well as various types of chromosomal rearrangements around the coding exons have been identified in patients with CD and ACD [Meyer et al., 1997; Gordon et al., 2009]. In addition to PRS, patients with CD manifest bowing of the long bones (campomelia), hypoplastic scapulae, pelvic malformations, a missing pair of ribs, clubfeet, and 46,XY gonadal dysgenesis. ACD represents a mild variant of CD lacking campomelia. Since PRS is present in most patients with CD and ACD [Gordon et al., 2009], SOX9 likely plays a particularly important role in the development of the mandible.

Recently, molecular defects in the far upstream and the far downstream region of *SOX9* have been identified in patients with isolated PRS. Jamshidi et al. [2004] and Jakobsen et al. [2007] identified balanced translocations of t(2;17) in familial and sporadic PRS cases, respectively, and found that the 17q breakpoints are located more than 1.0 Mb upstream of *SOX9*. Subsequently, Benko et al. [2009] identified variable genomic abnormalities (translocations, deletions, and a nucleotide substitution) at a position more than 1.0 Mb apart from *SOX9* in two sporadic and five familial cases with PRS. Furthermore, Benko et al. [2009] showed that the deletions and translocations included several highly conserved noncoding elements (HCNE) and the nucleotide substitution abolished the tissue-specific enhancer activity of one of these HCNEs (HCNE-F2). These data provide the first evidence that dysfunction of the very-long-range enhancer(s) of *SOX9* causes isolated PRS. However, there is no other report of patients with a molecular defect in the far upstream or the far downstream region of *SOX9*. Here, we report on a male patient with a complex genomic rearrangement in the 5′ region of *SOX9*. Clinical and molecular analyses of this patient provide further information on tissue-specific regulation of *SOX9*.

CLINICAL REPORT

This Japanese male was born at 38 weeks of gestation after an uncomplicated pregnancy and delivery. At birth, his length was 48.0 cm (−0.48 SD), weight 2.83 kg (−0.55 SD), and head circumference 32.0 cm (±0 SD). Immediately after birth, he was referred to our clinic because of respiratory distress and facial anomalies. He had hypoplastic mandible, cleft palate, and glossoptosis and was therefore diagnosed as having PRS. In addition, he showed bilateral clubfeet. Campomelia and tibial skin dimples were not observed.

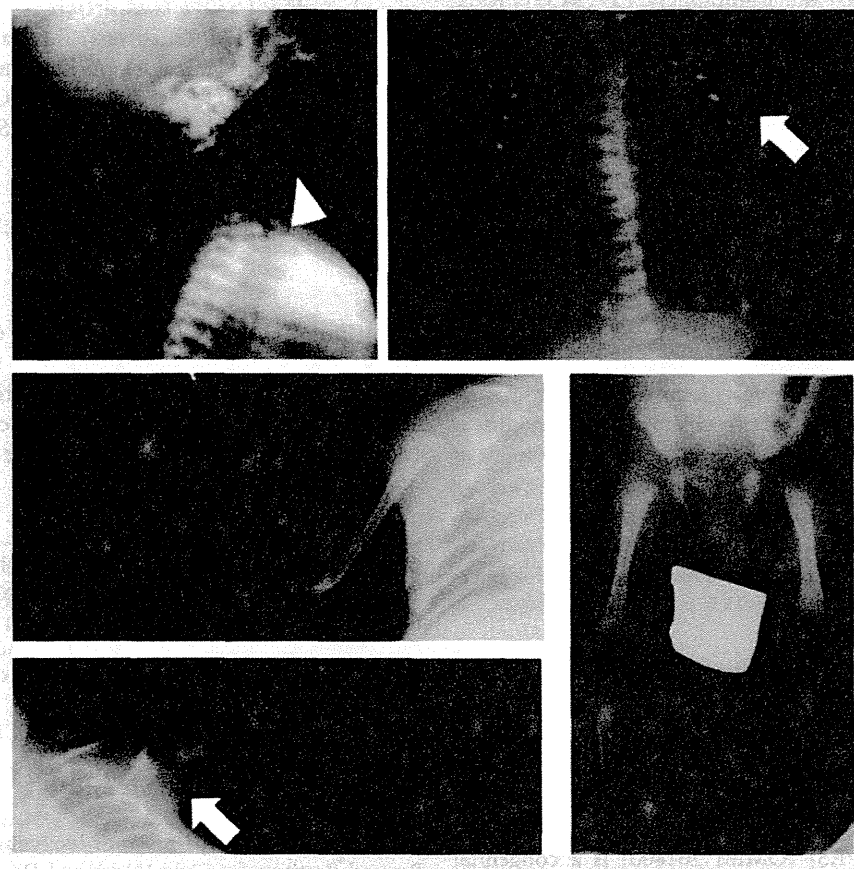

FIG. 1. Roentgenograms of the patient at 2 weeks of age. Mild hypoplasia of left scapula (white arrows) and micrognathia (a white arrowhead) are indicated.

He manifested normal male external genitalia with bilateral descended testes. On skeletal survey, dolichocephaly with hypoplasia of the facial bone, micrognathia, and hypoplasia of the left scapula were evident (Fig. 1). The right scapula was unremarkable. The ischia appeared somewhat broad, and the ischiopubic synchondroses wide; yet, these findings were too mild to be distinguishable from the normal range. Other radiological hallmarks in CD, such as cervical kyphosis, hypoplastic pedicles of the thoracic spine, and narrow ilia, were not discernible. G-banding chromosome analysis showed a normal 46,XY karyotype. Direct sequence analysis for *SOX9* detected no mutation in the coding region [Wada et al., 2009].

During several months after birth, he continually required medical intervention for respiratory and feeding difficulties. He underwent a tracheotomy at 8 months of age. He showed no obvious developmental delay; he was able to stand and walk along the wall at 1 year of age and was able to indicate his desires and needs by pointing at 1 year and 7 months of age. On his last examination at 1 year and 7 months of age, he measured 76.3 cm (−1.77 SD) and weighed 9.2 kg (−1.31 SD). His parents and sister were clinically normal.

MOLECULAR ANALYSES

This study was approved by the Institutional Review Board Committee at the National Center for Child Health and Development. After obtaining written informed consent from the parents, a peripheral blood sample was taken from the patient. Parental samples were not available for molecular analysis.

High-resolution chromosomal banding revealed a karyotype of 46,XY,der(17)inv(17)(q21.31q24.3)del(17)(q24.3q23?) (Fig. 2A). Fluorescence in situ hybridization (FISH) analysis using RP11-84E24-BAC containing *SOX9* and RP11-20N01-BAC on 17q21.31 indicated a paracentric inversion on one of the two chromosome 17 (Fig. 2B and C). Signals for *SOX9* were detected on two chromosome 17. Comparative genomic hybridization (CGH) analysis using a human genome oligoarray (1 × 1 M format, G4447A, Agilent Technologies, Palo Alto, CA) indicated a heterozygous deletion in the *SOX9* upstream region (Fig. 3A). In silico analysis using UCSC genome browser (http://genome.ucsc.edu/; hg 19; NCBI Build 37) showed that the deletion was 2.99 Mb in physical length and flanked by the proximal and the distal breakpoints residing at −4.15 and −1.16 Mb to *SOX9*, respectively. A total of 18 known genes were located within the deleted region, as assessed using the Refseq database (Fig. 3A).

DISCUSSION

A complex genomic rearrangement in the 5′ region of *SOX9* was identified in a boy with PRS. The genomic lesion started at a point 1.16 Mb upstream of *SOX9* and affected several HCNEs. In particular, HCNE-F2, previously shown to act as a developmental enhancer for the craniofacial region [Benko et al., 2009], was deleted in this patient (Fig. 3B). Thus, the PRS phenotype of this patient

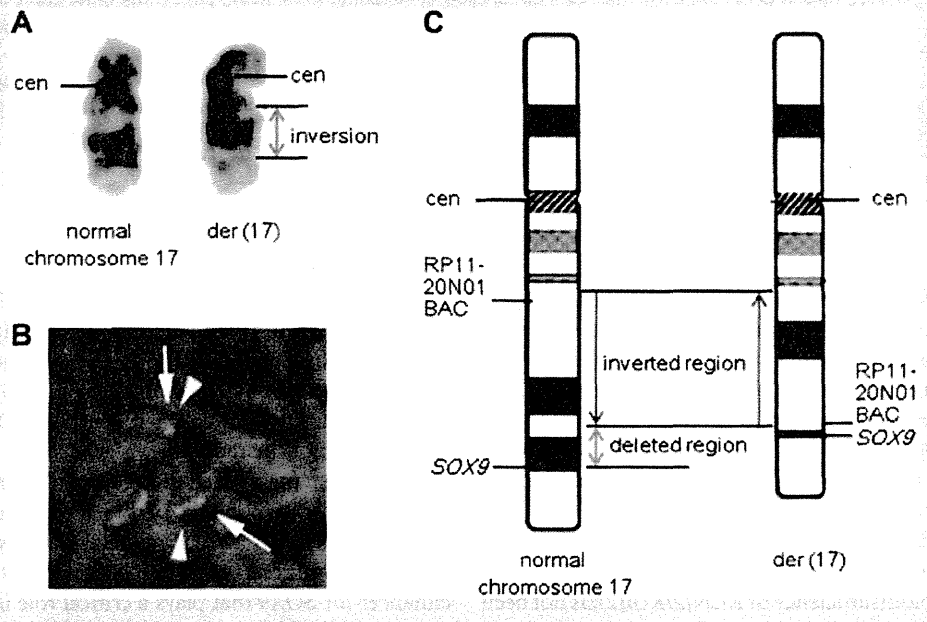

FIG. 2. Chromosomal banding and FISH analysis. A: High-resolution chromosomal banding indicating the presence of a deletion and an inversion on the long arm of chromosome 17. cen, centromere. B: Representative results of FISH analysis. The arrowheads denote RP11-84E24-BAC containing *SOX9* (green signals); the arrows indicate RP11-20N01-BAC on 17q21.31 (red signals). Two signals of an apparently different distance are present on two chromosome 17, indicating an inversion on one of two chromosome 17. Signals for *SOX9* are normally present on both chromosome 17. C: Schematic representation of the genomic rearrangement of the patient.

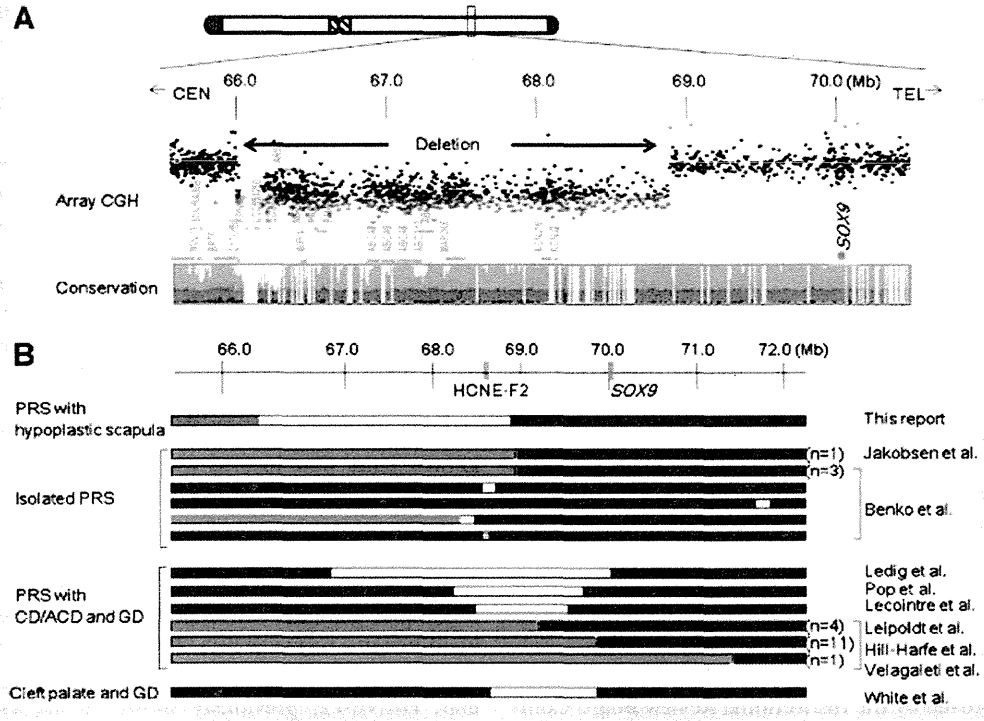

FIG. 3. Genomic abnormalities around *SOX9*. A: Oligoarray CGH analysis in the patient. The black, the red, and the green dots denote signals indicative of the normal, the increased (>+0.5), and the decreased (<−1.0) copy numbers, respectively. The deletion is 2.99 Mb in length and encompasses 18 Refseq genes and several highly conserved noncoding elements. The proximal border of the deletion is located at a point 1.16 Mb upstream of *SOX9*. Genomic positions are referred to the Human Genome (February 2009, hg 19; NCBI Build 37). B: Schematic representation of genomic lesions and clinical features of present case and previously reported patients [Pop et al., 2004; Hill-Harfe et al., 2005; Velagaleti et al., 2005; Jakobsen et al., 2007; Leipoldt et al., 2007; Benko et al., 2009; Lecointre et al., 2009; Ledig et al., 2010; White et al., 2011]. The white areas denote monosomic regions and the black areas, the disomic regions. The purple area indicates the inverted region. The blue regions in translocation-positive patients indicate DNA sequences derived from other chromosomes; the approximate location of translocation breakpoint clusters are shown in green, and the number of breakpoints within each cluster is shown in parenthesis. The gray region depicts a dosage-unknown region. The orange dot denotes a nucleotide substitution. HCNE-F2, the highly conserved noncoding element with enhancer activity reported by Benko et al. [2009]; PRS, Pierre Robin sequence; ACD, acampomelic campomelic dysplasia; GD, gonadal dysgenesis; CD, campomelic dysplasia.

would be ascribed to *SOX9* misexpression due to loss of HCNE-F2, although we cannot exclude the possibility of another hitherto unidentified *cis*-regulatory element(s) of *SOX9* being affected by the deletion/inversion. In this regard, while the deletion removed 18 genes, clinical features of the patient can be explained by *SOX9* dysfunction alone. Moreover, none of the 18 genes, except for *KCNJ2*, are known to be involved in mandibular growth. Furthermore, whereas dominant negative mutations of human *KCNJ2* as well as homozygous deletion of mouse *KcnJ2* have been shown to result in cleft palate and micrognathia [Zaritsky et al., 2000; Andelfinger et al., 2002], haploinsufficiency of *KCNJ2/KcnJ2* has not been shown to cause such abnormalities. Hence, the patient represents a novel case with PRS caused by a *SOX9 cis*-regulatory mutation. Such submicroscopic genomic rearrangements may also be present in other patients with isolated PRS. Indeed, only a few genes have been identified as causative genes for isolated PRS. In this regard, it is noteworthy that mutations of collagen genes including *COL11A2* and *COL11A1* have been shown to cause a PRS as a component of Stickler syndrome without apparent ocular involvement [Vikkula et al., 1995; Annunen et al., 1999]. Since collagen genes are known to be direct targets of SOX9 [Gordon et al., 2009], these data suggest that transactivation of collagen genes by SOX9 is critical for the development of the mandible.

This patient manifested PRS-compatible craniofacial abnormalities and mild hypoplasia of the left scapula. Nevertheless, he showed no typical CD/ACD skeletal features. These data indicate that the genomic rearrangement of the patient disrupted at least one enhancer for *SOX9* that plays a critical role in the development of the mandible and a small role in the development of the scapula. In addition, the concept of exclusion mapping implies that tissue-specific enhancers for long bones, pelvic bones, and ribs are located within the 1.16 Mb region closest to *SOX9*, because CD/ACD is known to be a fully penetrant phenotype in patients with intragenic mutations of *SOX9* [Meyer et al., 1997]. Consistent with this,

previous studies have suggested that putative loci for CD/ACD are located within the 1.0 Mb region from *SOX9* [Gordon et al., 2009]. Nevertheless, the phenotype of this patient could also be explained by assuming that there is a global developmental enhancer(s) of *SOX9* in the region more than 1.16 Mb apart from *SOX9* and that the mandible and the scapula are more sensitive to reduced transcriptional levels of *SOX9* than other skeletal tissues [Gordon et al., 2009]. Indeed, various skeletal changes of the patient such as clubfeet, borderline broad ischia, and relatively wide ischiopubic synchondroses, may be related to mildly impaired *SOX9* expression. In this context, it is noteworthy that CD, ACD, and isolated PRS are currently regarded as a continuum of a disorder caused by *SOX9* abnormalities [Gordon et al., 2009]. Thus, this patient may represent an intermediate phenotype between ACD and isolated PRS.

This patient had normal male external genitalia, indicating that the testis-specific enhancer(s) of *SOX9* is preserved in this patient. Consistent with this, previous studies on translocation-positive patients suggested that a testis-specific enhancer(s) is located within the 789 kb region closest to *SOX9* [Gordon et al., 2009]. Moreover, animal studies have identified a testis-specific enhancer immediately upstream of *Sox9* [Sekido and Lovell-Badge, 2008]. However, fairly well preserved masculinization of this patient may be ascribed to incomplete penetrance of gonadal dysgenesis in *SOX9* abnormalities, because normal testicular development has been observed in about 25% of 46,XY individuals with a *SOX9* intragenic mutation [Mansour et al., 1995].

To date, various types of cryptic deletions have been identified in patients with PRS (Fig. 3B). Notably, there is no overlapping region of deletion that is shared by all PRS cases, although the deletions of sporadic case 4 and familial case 1 reported by Benko et al. [2009] are located within the deleted region of the patient described herein. These results imply that multiple *cis*-acting elements around *SOX9* are required for the appropriate development of the mandible. Further analysis in a large cohort of PRS patients would enable us to clarify the precise locations of *SOX9* tissue-specific enhancers. In this regard, array CGH would serve as a powerful tool for screening of such patients, because it can detect various copy number alterations in a chromosomal region of several megabases.

In summary, the present study provides a novel example for long-range *cis*-regulatory mutations of *SOX9*. Our findings suggest that the genomic region more than 1.16 Mb upstream of *SOX9* includes at least one *cis*-acting element that regulates *SOX9* expression in the developing mandible, and, to a lesser extent, in the developing scapula. Further studies will permit the full characterization of the genomic environment involved in tissue-specific regulation of *SOX9*.

ACKNOWLEDGMENTS

This research was supported by the Grant-in-Aid for Scientific Research on Innovative Areas (22132004) from the Ministry of Education, Culture, Sports, Science and Technology (MEXT), by the Grant-in-Aid for Scientific Research (B) (23390249) from the Japan Society for the Promotion of Science (JSPS), the Grants for Research on Intractable Diseases (10103415) (11103332) from the Ministry of Health, Labor and Welfare and the Grant of National Center for Child Health and Development (23A-1).

REFERENCES

Andelfinger G, Tapper AR, Welch RC, Vanoye CG, George AL Jr, Benson DW. 2002. KCNJ2 mutation results in Andersen syndrome with sex-specific cardiac and skeletal muscle phenotypes. Am J Hum Genet 71:663–668.

Annunen S, Körkkö J, Czarny M, Warman ML, Brunner HG, Kääriäinen H, Mulliken JB, Tranebjaerg L, Brooks DG, Cox GF, Cruysberg JR, Curtis MA, Davenport SL, Friedrich CA, Kaitila I, Krawczynski MR, Latos-Bieleńska A, Mukai S, Olsen BR, Shinno N, Somer M, Vikkula M, Zlotogora J, Prockop DJ, Ala-Kokko L. 1999. Splicing mutations of 54-bp exons in the COL11A1 gene cause Marshall syndrome, but other mutations cause overlapping Marshall/Stickler phenotypes. Am J Hum Genet 65:974–983.

Benko S, Fantes JA, Amiel J, Kleinjan DJ, Thomas S, Ramsay J, Jamshidi N, Essafi A, Heaney S, Gordon CT, McBride D, Golzio C, Fisher M, Perry P, Abadie V, Ayuso C, Holder-Espinasse M, Kilpatrick N, Lees MM, Picard A, Temple IK, Thomas P, Vazquez MP, Vekemans M, Roest Crollius H, Hastie ND, Munnich A, Etchevers HC, Pelet A, Farlie PG, Fitzpatrick DR, Lyonnet S. 2009. Highly conserved non-coding elements on either side of SOX9 associated with Pierre Robin sequence. Nat Genet 41:359–364.

Gordon CT, Tan TY, Benko S, Fitzpatrick D, Lyonnet S, Farlie PG. 2009. Long-range regulation at the SOX9 locus in development and disease. J Med Genet 46:649–656.

Hill-Harfe KL, Kaplan L, Stalker HJ, Zori RT, Pop R, Scherer G, Wallace MR. 2005. Fine mapping of chromosome 17 translocation breakpoints >or= 900 kb upstream of SOX9 in acampomelic campomelic dysplasia and a mild, familial skeletal dysplasia. Am J Hum Genet 76:663–671.

Holder-Espinasse M, Abadie V, Cormier-Daire V, Beyler C, Manach Y, Munnich A, Lyonnet S, Couly G, Amiel J. 2001. Pierre Robin sequence: A series of 117 consecutive cases. J Pediatr 139:588–590.

Jakobsen LP, Ullmann R, Christensen SB, Jensen KE, Mølsted K, Henriksen KF, Hansen C, Knudsen MA, Larsen LA, Tommerup N, Tümer Z. 2007. Pierre Robin sequence may be caused by dysregulation of SOX9 and KCNJ2. J Med Genet 44:381–386.

Jamshidi N, Macciocca I, Dargaville PA, Thomas P, Kilpatrick N, McKinlay Gardner RJ, Farlie PG. 2004. Isolated Robin sequence associated with a balanced t(2;17) chromosomal translocation. J Med Genet 41:e1.

Lecointre C, Pichon O, Hamel A, Heloury Y, Michel-Calemard L, Morel Y, David A, Le Caignec C. 2009. Familial acampomelic form of campomelic dysplasia caused by a 960kb deletion upstream of SOX9. Am J Med Genet A 149:1183–1189.

Ledig S, Hiort O, Scherer G, Hoffmann M, Wolff G, Morlot S, Kuechler A, Wieacker P. 2010. Array-CGH analysis in patients with syndromic and non-syndromic XY gonadal dysgenesis: Evaluation of array CGH as diagnostic tool and search for new candidate loci. Hum Reprod 25: 2637–2646.

Leipoldt M, Erdel M, Bien-Willner GA, Smyk M, Theurl M, Yatsenko SA, Lupski JR, Lane AH, Shanske AL, Stankiewicz P, Scherer G. 2007. Two novel translocation breakpoints upstream of SOX9 define borders of the proximal and distal breakpoint cluster region in campomelic dysplasia. Clin Genet 71:67–75.

Mansour S, Hall CM, Pembrey ME, Young ID. 1995. A clinical and genetic study of campomelic dysplasia. J Med Genet 32:415–420.

Meyer J, Südbeck P, Held M, Wagner T, Schmitz ML, Bricarelli FD, Eggermont E, Friedrich U, Haas OA, Kobelt A, Leroy JG, Van Maldergem L, Michel E, Mitulla B, Pfeiffer RA, Schinzel A, Schmidt H, Scherer G.

1997. Mutational analysis of the SOX9 gene in campomelic dysplasia and autosomal sex reversal: Lack of genotype/phenotype correlations. Hum Mol Genet 6:91–98.

Pop R, Conz C, Lindenberg KS, Blesson S, Schmalenberger B, Briault S, Pfeifer D, Scherer G. 2004. Screening of the 1 Mb SOX9 5' control region by array CGH identifies a large deletion in a case of campomelic dysplasia with XY sex reversal. J Med Genet 41:e47.

Robin P. 1934. Glossoptosis due to atresia and hypertrophy of the mandible. Am J Dis Child 48:541–547.

Sekido R, Lovell-Badge R. 2008. Sex determination involves synergistic action of SRY and SF1 on a specific Sox9 enhancer. Nature 453:930–934.

Velagaleti GV, Bien-Willner GA, Northup JK, Lockhart LH, Hawkins JC, Jalal SM, Withers M, Lupski JR, Stankiewicz P. 2005. Position effects due to chromosome breakpoints that map approximately 900 kb upstream and approximately 1.3 Mb downstream of SOX9 in two patients with campomelic dysplasia. Am J Hum Genet 76:652–662.

Vikkula M, Mariman EC, Lui VC, Zhidkova NI, Tiller GE, Goldring MB, van Beersum SE, de Waal Malefijt MC, van den Hoogen FH, Ropers HH, Mayne R, Cheah KSE, Olsen BR, Warman ML, Brunner HG. 1995. Autosomal dominant and recessive osteochondrodysplasias associated with the COL11A2 locus. Cell 80:431–437.

Wada Y, Nishimura G, Nagai T, Sawai H, Yoshikata M, Miyagawa S, Hanita T, Sato S, Hasegawa T, Ishikawa S, Ogata T. 2009. Mutation analysis of SOX9 and single copy number variant analysis of the upstream region in eight patients with campomelic dysplasia and acampomelic campomelic dysplasia. Am J Med Genet A 149:2882–2885.

White S, Ohnesorg T, Notini A, Roeszler K, Hewitt J, Daggag H, Smith C, Turbitt E, Gustin S, van den Bergen J, Miles D, Western P, Arboleda V, Schumacher V, Gordon L, Bell K, Bengtsson H, Speed T, Hutson J, Warne G, Harley V, Koopman P, Vilain E, Sinclair A. 2011. Copy number variation in patients with disorders of sex development due to 46,XY gonadal dysgenesis. PLoS One 6:e17793.

Zaritsky JJ, Eckman DM, Wellman GC, Nelson MT, Schwarz TL. 2000. Targeted disruption of Kir2.1 and Kir2.2 genes reveals the essential role of the inwardly rectifying K(+) current in K(+)-mediated vasodilation. Circ Res 87:160–166.

Journal of Human Genetics (2012) 57, 449–452

www.nature.com/jhg

ORIGINAL ARTICLE

Haplotype analysis of *ESR2* in Japanese patients with spermatogenic failure

Tsutomu Ogata[1,2], Maki Fukami[2], Rie Yoshida[2], Eiko Nagata[1], Yasuko Fujisawa[1], Atsumi Yoshida[3] and Yasunori Yoshimura[4]

The prevalence of spermatogenic failure (SF) has gradually increased during the past few decades at least in several countries. Although multiple factors would be involved in this phenomenon, one important factor would be excessive estrogen effects via estrogen receptors (ERs). Thus, we performed haplotype analysis of *ESR2* encoding ERβ in 125 Japanese SF patients and 119 age-matched control males, using single nucleotide polymorphisms (SNPs) 1–9 that are widely distributed on the ~120-kb genomic sequence of *ESR2*. Consequently, a linkage disequilibrium (LD) block was detected in an ~60-kb region encompassing SNPs 2–7 in both groups, and four major estimated haplotypes were identified within the LD block. Furthermore, the most prevalent 'TGTAGA' haplotype was found to be significantly associated with SF, with the *P*-value obtained by the Cochran–Armitage trend test (0.0029) being lower than that obtained by a 100 000-times permutation test (0.0038) to cope with the problem of multiple comparisons. The results, in conjunction with our previous data indicating lack of a susceptibility factor on *ESR1* encoding ERα, imply that the specific 'TGTAGA' haplotype of *ESR2* raises the susceptibility to the development of SF.
Journal of Human Genetics (2012) **57,** 449–452; doi:10.1038/jhg.2012.53; published online 24 May 2012

Keywords: environmental endocrine disruptors; *ESR2*; estrogenic effects; haplotype analysis; spermatogenic failure; susceptibility

INTRODUCTION

Recent studies have indicated a gradual increase in the prevalence of male genial and reproductive abnormalities during the past few decades at least in several countries.[1] Skakkebaek *et al.*[2] have coined a term 'testicular dysgenesis syndrome' for this phenomenon. As such deterioration of male genital and reproductive health is also observed in many wildlife species,[1,3] it is likely that such adverse changes in males are inter-related events shared in common by the human and the wildlife species.[1,3] In this regard, environmental endocrine disruptors (EEDs) appear to constitute the major factor for this phenomenon, because EEDs are widely spread in the world.[1,3] In particular, exposure to estrogenic EEDs are known to affect male genital and reproductive health.[1,3–5]

The effects of EEDs would primarily be determined by the genetic susceptibility, together with the dosage of exposed EEDs, character of exposed EEDs (for example, estrogenic, anti-androgenic and so on), and the developmental stage of the individuals at the time of EED exposure.[1,3] In this regard, it is known that estrogenic EEDs can bind to both estrogen receptor (ER)α encoded by *ESR1* and ERβ encoded by *ESR2* with low but variable degrees of affinities.[3] Thus, it is likely that genetic susceptibility to estrogenic EEDs is primarily constituted by genetic variations in *ESR1* and *ESR2*.[1,3]

To examine this possibility, we have previously performed haplotype analysis of *ESR1* in Japanese male patients with genial and reproductive abnormalities as well as in control males, using 15 single nucleotide polymorphisms (SNPs 1–15) that are widely distributed throughout the >300-kb genomic sequence of *ESR1*.[6,7] Consequently, we identified an ~50-kb linkage disequilibrium (LD) block spanning SNPs 10–14 in the 3′ region of *ESR1*, and found that homozygosity of a specific 'AGATA' haplotype within the LD block was strongly associated with cryptorchidism ($P=0.0040$; odds ratio (OR) = 7.55) and hypospadias ($P=0.000057$; OR = 13.75)[6,7] (and our unpublished updated observation). This finding provides strong evidence that homozygosity of the specific *ESR1* haplotype raises the susceptibility to the development of male genital abnormalities. In this context, we speculate that this effect via the specific *ESR1* haplotype is mediated by EEDs, although there is no direct evidence yet. Indeed, as *ESR1* is expressed in Leydig cells producing testosterone and insulin-like 3,[5,8] it is likely that the specific *ESR1* haplotype primarily enhances estrogenic effects in Leydig cells, compromising their hormonal production capacity.

However, no significant association was found between the specific 'AGATA' haplotype of *ESR1* and spermatogenic failure (SF).[7] In this context, as *ESR2* is clearly expressed in various developmental stages of male germ cells,[5] it may be possible that the deleterious effects of estrogenic EEDs on spermatogenesis may primarily be mediated by ERβ. Thus, we carried out haplotype analysis of *ESR2* in Japanese patients with SF.

[1]Department of Pediatrics, Hamamatsu University School of Medicine, Hamamatsu, Japan; [2]Department of Molecular Endocrinology, National Research Institute for Child Health and Development, Tokyo, Japan; [3]Kiba Park Clinic, Tokyo, Japan and [4]Department of Obstetrics and Gynecology, Keio University School of Medicine, Tokyo, Japan
Correspondence: Professor T Ogata, Department of Pediatrics, Hamamatsu University School of Medicine, 1-20-1, Handayama, Higashi-ku, Hamamatsu, Shizuoka 431-3192, Japan.
E-mail: tomogata@hama-med.ac.jp
Received 28 November 2011; revised 25 April 2012; accepted 28 April 2012; published online 24 May 2012

MATERIALS AND METHODS

Subjects

We studied 125 SF patients aged 32–52 years (median 41.0 years), including 80 SF patients utilized in the previous *ESR1* haplotype analysis.[7] The selection criteria included: (1) azoospermia or severe oligozoospermia (<5 million sperms per ml) demonstrated by two consecutive analyses of semen obtained after 4–7 days of abstinence; (2) lack of extragenital anomalies such as cryptorchidism and hypospadias; (3) hypergonadotropic hypogonadism indicative of primary testicular dysfunction; (4) no seminal tract obstruction, varicocele, or retrograde ejaculation; (5) a 46,XY karyotype with no demonstrable structural or numerical abnormality after examining ⩾30 lymphocytes; (6) absence of a Y chromosomal microdeletion after examining 36 loci from *SRY* to *DYZ1*, including multiple Yq loci in the azoospermia factor regions (AZFa, b, c) such as *RBMY* and *DAZ*;[9] (7) no significant expansion of CAG repeat length at exon 1 of *AR* that is known to raise the susceptibility to male reproductive abnormalities;[10] and (8) lack of a disease episode that could affect fertility such as mumps orchiditis. For controls, 119 control adult males with proven fertility aged 24–50 years (median 35.5 year) were similarly analyzed with permission. The ages were similar between the SF patients and control males (Mann–Whitney's *U*-test). All the SF patients and control males were Japanese living in the Tokyo urban area; they were free from particular residential environments such as the vicinity of chemical factories or farms, from specific dietary habits deviated to vegetables or animal/fish proteins, and from intake of drugs with hormonal effects.

SNP analysis

This study was approved by the Institutional Review Board Committees of the authors, and informed consent was obtained from each subject. We examined nine SNPs (SNPs 1–9) that were associated with high minor allele frequencies in the Japanese population (20.3–39.5%) (the NCBI Short Genetic Variations Database (dbSNP); http://www.ncbi.nlm.nih.gov/snp/) and were widely distributed on the ~120-kb *ESR2* genomic DNA sequence including an apparent LD block encompassing exons 1–6 identified in various populations (the International HapMap Project Database; http://hapmap.ncbi.nlm.nih.gov/) (Figure 1a). Genotyping was performed by the 5′ nuclease assay on an ABI PRISM 7000 Sequence Detection System (Life Technologies, Carlsbad, CA, USA),[11] using leukocyte genomic DNA of each subject.

Pearson's χ^2-test with one degree of freedom was applied to test whether the genotyping data are in the Hardy–Weinberg equilibrium. Statistical significance of the differences in allele and genotype frequencies was analyzed by Pearson's χ^2-test, using R environment for statistical computing (http://www.r-project.org/).

Haplotype analysis

Although haplotypes are usually not observed, the haplotypes present in a subject and the frequencies of the haplotypes in a population can be inferred using genotype data at separate loci.[12] In this regard, the degree of LD can be expressed as the pairwise $|D'|$ value (the absolute value for the disequilibrium parameter) that ranges from 0 (complete absence of LD) to 1.0 (complete presence of LD),[13] and a chromosomal region associated with high $|D'|$ values between different loci is defined as a haplotype or an LD block.[14] In this study, haplotype inference was performed by the maximum-likelihood method using expectation maximization algorithm implemented in the software LDSUPPORT.[15,16] The pairwise $|D'|$ values were estimated by the method of Terwilliger and Ott, [12] and a haplotype block was determined by the method of Zhu *et al.*[17] using the software developed by Kamatani *et al.*[18]

The difference in the frequencies of haplotypes between the SF patients and the control males was examined using the estimated population haplotype frequencies by Pearson's χ^2-test, and the OR and the 95% confidence interval (CI) were calculated using the R environment. The association between SF phenotype and estimated haplotypes was tested using PENHAPLO software in a dominant mode (comparison of the frequencies of subjects with one risk haplotype between cases and controls) and in a recessive mode (comparison of the frequencies of subjects with two risk haplotypes between cases and controls).[19] Furthermore, the association between SF phenotype and estimated haplotypes was also examined in a dosage-dependent mode (comparison of the frequencies of subjects with zero, one, and two risk haplotypes between cases and controls) by the Cochran–Armitage trend test,[20,21] using the R environment. To cope with the problem of multiple comparisons, the significant level was determined by a 100 000-times permutation test.[22]

RESULTS

SNP analysis

The results of SNP analysis are summarized in Table 1. Minor allele frequencies of the 9 SNPs were 20.4–46.8% in the SF patients and 27.7–37.3% in control males. The genotype frequencies of SNPs 1–9 were in accord with the Hardy–Weinberg equilibrium. Low *P*-values (<0.05) were identified for the differences in the allele and genotype frequencies of SNPs 1, 4, and 5, with stronger association being identified for the

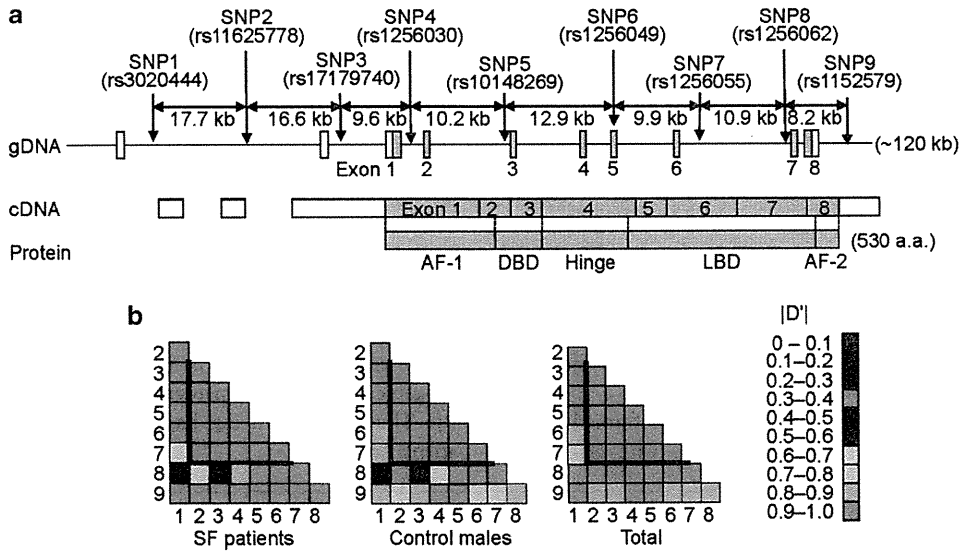

Figure 1 Schematic representation of *ESR2* and its LD maps. (**a**) Physical positions of *ESR2* SNPs 1–9 examined in the present study. The gray and the white boxes represent coding and untranslated regions, respectively. AF-1, activation function 1 (ligand independent); AF-2: activation function 2 (ligand dependent); DBD, DNA-binding domain; LBD, ligand-binding domain. (**b**) Pairwise LD maps. $|D'|$: an absolute value for the disequilibrium parameter.

Table 1 Summary of SNP analysis

Genotyping data				*Statistical data*			
	Genotype	*SF*	*CM*		*P-value*	*OR*	*95% CI*
SNP1	TT	78	58	T vs C	0.028	1.59	1.05–2.42
rs3020444	TC	43	53	TT vs TC + CC	0.032	0.57	0.34–0.95
	CC	4	8	TT + TC vs CC	0.20	2.18	0.64–7.44
SNP2	TT	68	63	T vs C	0.74	1.07	0.72–1.56
rs11625778	TC	48	46	TT vs TC + CC	0.82	0.94	0.57–1.56
	CC	9	10	TT + TC vs CC	0.73	1.18	0.46–3.02
SNP3	GG	77	59	G vs A	0.059	1.49	0.98–2.25
rs17179740	AG	43	52	GG vs AG + AA	0.059	0.61	0.37–1.02
	AA	5	8	GG + AG vs AA	0.34	1.73	0.55–5.45
SNP4	CC	36	55	C vs T	0.0022	1.77	1.23–2.56
rs1256030	CT	61	49	CC vs CT + TT	0.0049	2.13	1.25–3.61
	TT	28	15	CC + CT vs TT	0.045	0.500	0.25–0.99
SNP5	GG	36	55	G vs A	0.0022	1.77	1.23–2.56
rs10148269	AG	61	49	GG vs AG + AA	0.0049	2.13	1.25–3.61
	AA	28	15	GG + AG vs AA	0.045	0.500	0.25–0.99
SNP6	GG	68	64	G vs A	0.74	1.07	0.72–1.60
rs1256049	GA	49	45	GG vs GA + AA	0.92	0.98	0.59–1.61
	AA	8	10	GG + GA vs AA	0.55	1.34	0.51–3.52
SNP7	AA	68	64	A vs G	0.74	1.07	0.72–1.60
rs1256055	AG	49	45	AA vs AG + GG	0.92	0.98	0.59–1.61
	GG	8	10	AA + AG vs GG	0.55	1.34	0.51–3.52
SNP8	AA	59	47	A vs G	0.21	1.27	0.87–1.85
rs1256062	AG	54	57	AA vs AG + GG	0.22	0.73	0.44–1.21
	GG	12	15	AA + AG vs GG	0.45	1.36	0.61–3.04
SNP9	GG	40	45	G vs A	0.12	1.34	0.93–1.92
rs1152579	GA	59	59	GG vs GA + AA	0.34	1.29	0.76–2.19
	AA	26	15	GG + GA vs AA	0.087	0.55	0.28–1.10

Abbreviations: CI, confidence interval; OR, odds ratio; SNP, single nucleotide polymorphism. NCBI rs no. is given for each SNP. SF, 125 patients with spermatogenic failure; CM, 119 control males.

allele rather than the genotype frequencies. In particular, the *P*-values for allele frequencies of SNPs 4 and 5 were markedly low.

Haplotype analysis

The LD map is shown in Figure 1b, and the results of haplotype analysis are summarized in Table 2. An ~60-kb LD block spanning SNPs 2–7 was identified in both the SF patients and control males, with the $|D'|$ value being >0.9 for all the pairs of SNPs 2–7. Within the LD block, four major estimated haplotypes were identified, together with three additional minor haplotypes ('CGTAGA' haplotype in a single control male, and 'TATAGA' and 'CGCGGA' haplotypes in single SF patients). Notably, the frequency of the most prevalent 'TGTAGA' haplotype was significantly higher in the SF patients than in the control males. Furthermore, the 'TGTAGA' haplotype was significantly associated with SF phenotype, with the *P*-value obtained by the Cochran–Armitage trend test (0.0029) being lower than the permutation *P*-value (0.0038). In addition, of the four major haplotypes, the 'TGTAGA' haplotype alone contained the 'T' allele in SNP 4 and the 'A' allele in SNP 5, whereas these two alleles were also identified in two of the three minor haplotypes.

DISCUSSION

The present study revealed the presence of an ~60-kb LD block encompassing SNPs 2–7 of *ESR2* in both the SF patients and control males. In this regard, the allele frequencies obtained in the control males are comparable to those registered in the JSNP Database, and the LD

Table 2 Summary of haplotype analysis (SNPs 2–7)

Estimated haplotype	*TGTAGA*	*TACGGA*	*CGCGAG*	*TGCGGA*
SF (n = 125)	46.4%	21.2%	26.0%	6.0%
CM (n = 119)	32.7%	28.1%	27.3%	11.0%
Comparison of estimated haplotype frequency				
P-value	0.0028	0.096	0.82	0.070
OR	1.77	0.69	0.94	0.52
95% CI	1.21–2.61	0.44–1.06	0.61–1.43	0.25–1.05
Association of estimated haplotype with phenotype				
Dominant mode				
P-value	0.0063	0.078	0.92	0.031
OR	2.08	0.63	0.98	0.46
95% CI	1.23–3.54	0.38–1.05	0.59–1.62	0.22–0.93
Recessive mode				
P-value	0.026	0.34	0.55	0.97
OR	2.16	0.58	0.75	0.95
95% CI	1.09–4.46	0.17–1.79	0.28–1.96	0.037–24.2
Cochran–Armitage's trend test				
P-value	0.0029	0.071	0.75	0.056
For one haplotype				
OR	1.75	0.67	0.94	0.52
95% CI	1.21–2.52	0.44–1.03	0.63–1.39	0.27–1.02
For two haplotypes				
OR	3.06	0.45	0.88	0.27
95% CI	1.46–6.35	0.19–1.06	0.39–1.93	0.07–1.04

Abbreviations: CI, confidence interval; OR, odds ratio; SNP, single nucleotide polymorphism. SF, 125 patients with spermatogenic failure; CM, 119 control males.

block identified in this study is similar to that reported in the International HapMap Project. These findings argue for the accuracy of our data.

Of the four major estimated haplotypes within the LD block, the 'TGTAGA' haplotype was significantly associated with SF. Indeed, the *P*-value obtained by the Cochran–Armitage trend test was below the permutation *P*-value. Furthermore, comparison of the *P*-values obtained from the three types of analyses for the association between SF phenotype and estimated haplotypes implies that the specific 'TGTAGA' haplotype compromises spermatogenesis in a dosage-dependent manner rather than in a simple dominant or recessive manner. In this regard, as the 'T' allele of SNP 4 and the 'A' allele of SNP 5 are almost exclusively present in the 'TGTAGA' haplotype, genotyping of SNPs 4 and 5 can be utilized for the screening of the 'TGTAGA' haplotype.

For *ESR2*, previous studies have suggested an association between SF and an *Rsa*I SNP on exon 5 that does not result in amino acid change (SNP 6 in this study) in Scandinavian and Iranian populations (*P*-value: 0.01 and 0.012, respectively).[23,24] In such studies, as the frequency of AG genotype relative to GG genotype was higher in SF patients than in control males (AA genotype was extremely rare), this would imply that the 'A' allele of SNP 6 is regarded as a marker for a hidden true susceptibility factor(s) that is probably in an LD status with the 'A' allele of SNP 6. By contrast, the present study showed no association of SF with SNP 6 and rather suggests a dosage effect of the specific haplotype harboring the 'G' allele of SNP 6. Thus, the present data are apparently inconsistent with the previous studies. It might be possible, however, that the true susceptibility factor(s) is linked with the specific 'TGTAGA' haplotype in the Japanese population and resides on a different pattern of haplotype carrying the 'A' allele of SNP 6 in Scandinavian and Iranian populations, because of a recombination between the true susceptibility factor(s) and SNP 6 in either of the ethnic groups. In addition, there might be population-